ACKNOWLEDGMENTS

The authors would like to thank Dr. H. C. Britt for many helpful and stimulating discussions. The staff of the computing center at the Los Alamos Scientific Laboratory has been unfailingly helpful. We would particularly like to thank F. D. Newcom and Mrs. Evelyn Griggs for their help in preparing the manuscript. One of us (M.J.B.) would like to thank Professor R. K. Sheline and Dr. H. T. Motz for their encouragement and support in writing this paper.

PHYSICAL REVIEW VOLUME 156, NUMBER 4 20 APRIL 1967

Emission of Long-Range Alpha Particles in the Spontaneous Fission of Cf^{252}†

Z. FRAENKEL

Lawrence Radiation Laboratory, University of California, Berkeley, California
and
*Weizmann Institute of Science, Rehovoth, Israel**

(Received 23 September 1966; revised manuscript received 15 December 1966)

An experimental investigation of α-particle emission in the spontaneous fission of Cf^{252} is described. The measured angular distribution and energy distribution of the α particles are presented, as well as the mass-ratio distribution of the fission fragments and the single-fragment energy distribution in fission accompanied by long-range α particles (LRA fission). Also shown is the angular distribution of the α particles as a function of the α-particle energy, the total fission-fragment energy, and the mass ratio. The experimental results show the LRA-fission process to be very similar to binary fission until the moment of scission. The angular distribution of the α particles as a function of the mass ratio (corrected for α-particle recoil) confirms the earlier conclusion that the scission point moves towards the light fragment as the mass ratio increases. The experimental results provide evidence that the α particle is emitted very close to the scission point and within 10^{-21} sec of the moment of scission. The angular distribution data support the model which explains the variation of the number of neutrons emitted in binary fission as a function of fragment mass on the basis of a variation in the nuclear deformation of the fission fragments at scission.

I. INTRODUCTION

THE occasional emission of a high-energy α particle during the fission process was first observed by Alvarez.[1] Most of the early work on this process was done with the aid of photographic plates, and therefore it was generally called long-range alpha fission (LRA fission for short). Since it occurs only once in approximately 400 fission events (this number varies according to the fissioning nucleus and its excitation energy), the accurate measurement of LRA fission presented great experimental difficulties, and its relative rareness did not give much hope that it would greatly help in the understanding of the fission process in general.

Recently the research activity in the LRA-fission process has considerably increased. One of the reasons for this renewed activity is the advent of the solid-state detectors which can be used for the detection of both the fission fragments and the α particles with good energy and angular resolution. Another important reason for the renewed activity is the recent development of multidimensional pulse-height analyzers.

One of the most important facts to note about the emission of high-energy α particles in the fission process is the angular distribution, which is peaked in the direction perpendicular to the direction of the fission fragments.[2] This experimental fact leads one to believe that the α particle is emitted very close to the moment of scission when the two fragments separate. It is assumed that the α particle is emitted from the "neck" connecting the two fission fragments, most probably at the point at which the neck ruptures.[3] The sharply peaked angular distribution can then be explained by the effect of the electrostatic fields of the two fission fragments on the α particle. This rather accurate localization of the moment of its emission and the point at which it is emitted makes the α particle a possible tool for the study of the configuration of the nucleus at the moment of scission. Thus it may be said that one of the major reasons for our interest in LRA fission is the use of the α particles as a "probe" of the nuclear configuration at the moment of scission. The detailed examination of the α-particle distribution in LRA fission gives us direct information on the shape of the nucleus at scission. In principle the shape of the nucleus can be determined in considerable detail, provided that the

† Research performed in part under the auspices of the U. S. Atomic Energy Commission.

* Present address: The Weizmann Institute of Science, Rehovoth, Israel.

[1] L. W. Alvarez as reported by G. Farwell, E. Segrè, and C. Wiegand, Phys. Rev. **71**, 327 (1947).

[2] E. W. Titterton, Nature **168**, 590 (1951).

[3] Tsien San-Tsiang, J. Phys. Radium **9**, 6 (1949).

angular and energy distributions of the α particles are determined with the necessary accuracy and that detailed calculations are performed on the shape of the nucleus at scission which would give rise to these distributions.

Another way of gaining information on the shape of the nucleus at the moment of scission is the detailed study of the number of neutrons emitted from the fission fragments as a function of the fragment mass (the so-called "Terrell curve").[4] By measuring both the number of neutrons and their energy, we can determine the excitation energy of the fragments. In low-energy fission most of this energy was at the moment of scission in the form of deformation energy of the fragments. Thus we might gain information on the deformation of the nucleus at scission from the examination of subsequent neutron evaporation from the fragments. The study of neutron evaporation gives us only indirect information on the nuclear deformation at scission since we have to "translate" excitation energy (which is measured by measuring neutron emission) into nuclear deformation. We must therefore know the relation between those two quantities, i.e., the nuclear "stiffness" coefficient. Moreover, from neutron evaporation we obtain only one number which is correlated to the total deformation of the fragment at the moment of scission, and we have no hope of obtaining information on the exact shape of the fragment at scission by knowing only its total deformation energy. While this fact greatly restricts the amount of information on the shape of the nucleus at the moment of scission which we can obtain from neutron emission, a direct correlation exists between the excitation energy as measured by neutron evaporation and the total deformation of the fragment at scission. No such unambiguous relation exists for LRA fission. In fact any interpretation of the LRA distributions in terms of the detailed nuclear configuration at the moment of scission must necessarily be to some extent ambiguous. The situation may thus be summarized by saying that while much more information on the shape of the nucleus at scission can be obtained from the study of LRA fission as compared to neutron emission, it is impossible to obtain this information unambiguously. This does not mean that no useful information can be obtained from an investigation of LRA fission without undue amount of numerical calculations. In a previous paper[5] we have shown that very important information on the scission configuration can be obtained by a mere inspection of the angular distribution of the α particles as a function of the mass ratio without performing any calculation. Similarly, Halpern[6] has been able to obtain quantitative estimates of the distance between the fragments and of the kinetic energy at the moment of scission without performing any detailed calculations. Yet is should be remembered that any interpretation of the experimental results of LRA fission in terms of the nuclear shape at scission is in general not unique even when accompanied by detailed calculations, and hence such interpretations should be approached with the proper caution.

We may also hope that by comparing information obtained on the deformation of the fragment at scission from the investigation of LRA fission with data obtained from neutron emission it will be possible to increase our knowledge on the nuclear stiffness. The best way to obtain pertinent data for such a comparison is to measure simultaneously the neutron yield and the α-particle energy and angular distribution. An experiment of this kind is presently under way.

In this paper we report on a detailed investigation of the properties of the α particles which are emitted once in 300 fission events[7] in the spontaneous fission of Cf^{252}. A preliminary report on this work has already been published.[5] In Sec. II we describe the experimental apparatus and procedure which were used in the experiment. In Sec. III we show the detailed experimental results which were analyzed with the aid of a computer to yield the correlation between the various variables which were measured in the experiment. Our interpretation of the results in terms of the nuclear configuration at scission is also given for some experimental results. In Sec. IV we summarize our conclusions. These are based mainly on the experimental results presented in Sec. III. In the same section we also discuss briefly the differences between the nuclear configuration at the moment of scission in binary and LRA fission.

II. EXPERIMENTAL APPARATUS AND PROCEDURE

The experimental arrangement is shown in Fig. 1. It consisted of a vacuum chamber of approximately 30-cm diameter which contained the source and the solid-state detectors for the measurement of the fission fragments and the α particles. The source consisted of Cf^{252} which was transferred by the self-transfer method on a backing of 100 $\mu g/cm^2$ Ni foil of 1.3-cm diameter. The source strength was 1.54×10^7 fissions/min. Another 100-$\mu g/cm^2$ foil was placed in front of the source. The main reason for the second foil was prevention of the contamination of the chamber by self-transfer from the Cf^{252} source. It had the additional advantage of making the source symmetrical with respect to the two fission fragments, each of which traversed one Ni foil before reaching the detector. The two fission-fragment counter assemblies consisted each of two guard-ring P-diffused solid-state detectors of 2.5-cm diam (1700-Ω cm base material) connected in parallel and placed on top of each other. The purpose of this arrangement was to increase the coincidence rate without impairing the

[4] J. Terrell, Phys. Rev. **127**, 880 (1962).
[5] Z. Fraenkel and S. G. Thompson, Phys. Rev. Letters **13**, 438 (1964).
[6] I. Halpern, CERN Report 1963 (unpublished).
[7] R. A. Nobles, Phys. Rev. **126**, 1508 (1962).

angular resolution too much. (Rectangular 1×2 cm detectors would have done equally well, and indeed would have simplified the corrections for the finite detector size in the angular distributions, but such detectors were not available.) Care was taken that the two detectors which were connected in parallel came from the same production batch and had similar characteristics. The α-particle counter assembly consisted of two Li-drifted Si detectors of 1-cm diam placed on top of each other and connected in parallel. Li-drifted detectors were used because at the time P-diffused or surface-barrier detectors with a sufficiently deep depletion layer to stop 30-MeV α particles were not available. All detectors were locally manufactured. The distance of the fission-fragment counters from the source was 4.0 cm, and that of the α-particle counter was 2.5 cm. The position of the fission-fragment counters was fixed, whereas the α-particle counter could be rotated around the source without breaking the vacuum. Because of space limitations the angle of the α-particle counter with respect to each fission-fragment detector could only be changed between 60° and 120°. Similarly, the Cf^{252} source could be rotated and its height changed from the outside. An absorber comprising several thin gold leaves of total thickness 16 mg/cm^2 was placed in front of the α-particle counter. Its purpose was to absorb the 6.1-MeV α particles from the α decay of Cf^{252}. These α particles are more abundant by a factor of 10^4 than the α particles from LRA fission, and would have otherwise created serious pulse pile-up and random-coincidence problems. The disadvantage of using an absorber was that no LRA-fission event of α energy below 6.1 MeV would be detected. In practice LRA-fission events with α-particle energy below 10 MeV were not used in the analysis. This was due to the natural straggling of the α particles in the absorber and also to holes in the absorber foils, as a result of which not all 6.1-MeV α particles were absorbed in the gold absorber. Another factor which made a lower limit of 10 MeV desirable was that at this level random coincidences between binary fission events and 6.1-MeV α particles from Cf^{252} contamination of the α counter were not counted. Such α particles would have appeared identical to 9.5-MeV α particles which traversed the gold absorber. It was therefore decided to use 10 MeV as a lower limit. With a much faster coincidence system, we might have been able to reduce this limit to 9 MeV. The actual coincidence resolving time used in the experiment was $2\tau=0.7$ μsec. The gold absorber was placed at the end of a rotating arm, on the other end of which was a small Es^{253}+Am^{241} source on thick backing. By rotating the absorber by 180° this source was brought in front of the α-particle detector. The two α-particle lines at 6.63 MeV (Es^{253}) and at 5.48 MeV (Am^{241}) served as calibration points for the α-particle counter. This calibration was particularly necessary in view of the window of approximately 0.25 MeV of the Li-drifted detectors. The fission-fragment counters were calibrated using the two peaks of the single-fragment energy distribution in binary fission of Cf^{252}. The energy values for the two peaks were taken from the time-of-flight measurement of Fraser *et al.*[8]

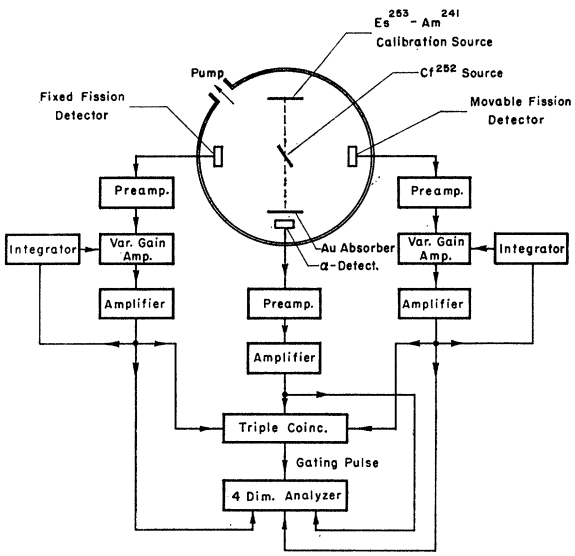

FIG. 1. Block diagram of the experimental apparatus.

The electronic system consisted of a charge-sensitive preamplifier followed by an amplifier for each of the three counters. The outputs of the amplifiers were fed into a triple-coincidence circuit and into a four-dimensional multichannel analyzer. The fourth dimension of the analyzer was utilized for calibration and checking purposes: At fixed intervals, a pulse generator fed standard pulses into the three preamplifiers, and also directly into the fourth dimension of the analyzer. This arrangement made possible a detailed check of the proper functioning of the electronic system. The calibration events could be identified as such during analysis by checking the contents of the calibration dimension.

The singles counting rates in the two fission-fragment counters were approximately 1.5×10^5 counts/min. Because of the lack of collimation of the source, only 40% of the above counts were coincidence counts of the two counters. The singles counting rate of the α counter was approximately 500 counts/min, and the triple-coincidence rate was approximately 8.5 counts/min for an angle of 90° between the fission and α counters. The random-coincidence rate was 0.35 counts/min, i.e., approximately 4% of the true rate at 90°. The random coincidences contributed an isotropic background to the angular distribution. The contribution to the coincidence rate due to background (i.e., true coincidences due to the contamination of one of the fission counters)

[8] J. S. Fraser, J. C. D. Milton, H. R. Bowman, and S. G. Thompson, Can. J. Phys. 41, 2080 (1963).

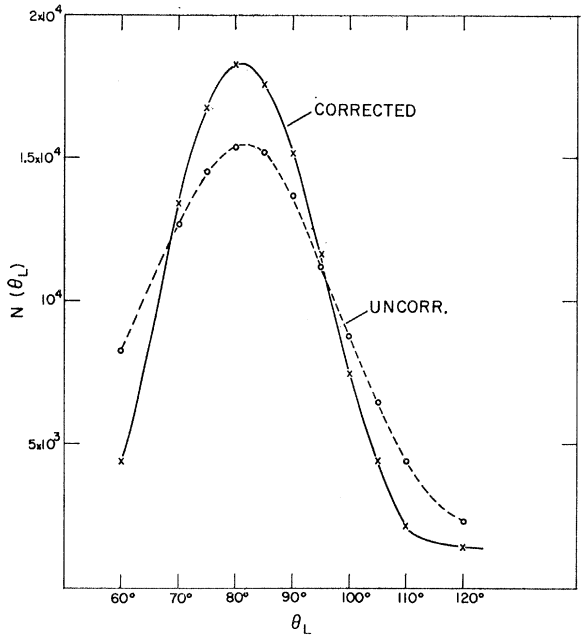

FIG. 2. The angular distribution of the α particles with and without corrections for the finite size of the detectors and the source.

was found too small to be measurable. Pulse pile-up presented no problem in the preamplifier-amplifier system. However, it led to some loss of the fission-fragment energy resolution due to the relatively large dead time of the multidimensional analyzer. The analyzer first stored the pulses in "stretcher circuits" and then analyzed each dimension sequentially. Pulse pile-up is probably mainly responsible for the 10% increase in the width of the total fission-fragment kinetic-energy distribution as compared with the width measured by the time-of-flight method of Fraser *et al.*[8]

The total recoil angle of the fission fragments due to the momentum of the α particle is 4.5° for an α particle of 16 MeV emitted at 90° with respect to the two fragments. Since this angle was well within the opening angle subtended by the counters, no correction due to this recoil had to be applied to the energy and angular distributions of the α particle.

The most serious problem encountered in the experiment was the deterioration of the fission-fragment detectors due to the large flux of fission fragments to which they were subjected. It has generally been accepted that solid-state detectors may receive as many as 10^9 fission fragments before seriously deteriorating. While this is obviously only an order-of-magnitude estimate (the actual limits depend very much on the type of base material used, the bias voltage, and other experimental factors), this number was found to be approximately correct for our detectors and experimental conditions. Since the detectors received approximately 2×10^8 fission fragments per day, they were changed every five days, by which time they were generally found to have seriously deteriorated. The deterioration manifested itself primarily in the increase of the leakage current and this resulted in a decrease of the effective gain of the preamplifier. Only at a later stage of the deterioration process did the change in energy resolution become serious. (It should be pointed out that a high-energy resolution of the fission-fragment detectors was not of primary importance in this experiment.) In order to overcome the decrease in gain, an "automatic gain control" system was installed in the two fission-counter circuits. This system operated in the following way: An integrator circuit counted all pulses above a certain discrimination level and the output of the integration circuit was fed back into a variable-gain amplifier placed between the preamplifier and main amplifier of that dimension. The variable-gain amplifier adjusted the forward gain so as to yield a constant integrator output. The point of discrimination of the integrators was chosen to be the high-energy peak of the fission spectrum, this point being the most sensitive one for such a system.

The angular distributions were obtained by measuring the number of coincidence counts at the following angles with respect to each fission-fragment detector: 60°, 70°, 75°, 80°, 85°, 90°, 95°, 100°, 105°, 110°, 120°. Since measurements at angles θ and $(180°-\theta)$ should yield identical results if the role of the two fission-fragment counters is interchanged, measurements in only one quadrant would have sufficed for obtaining the angular distributions. The measurements in the other quadrant were used to check the consistency of the data. During the measurements, the plane of the source foil was always at 30° with respect to the plane of the fission-fragment detectors. Of the four possible ways to satisfy this condition, the ones which yielded an angle of less than 60° between the plane of the source and the plane of the α-particle detector were chosen, i.e., when the α-particle counter was moved from one quadrant into the other the source was rotated by 60°. The fission-fragment counters always faced the same side of the source during any experimental run.

Our experimental system did not differentiate between α particles and other $Z\geq2$ particles emitted in the fission process. The "α-particle" events do therefore include a small fraction of events in which other $Z\geq2$ particles were emitted.[9,10] Our system was, on the other hand, insensitive to $Z=1$ particles,[7,9–13] since such particles with energy above 10 MeV were not stopped in the depletion layer of the α-particle detector, and our system did not record particles with kinetic energy below 10 MeV.

---

[9] S. L. Whetstone, Jr. and T. D. Thomas, Phys. Rev. Letters **15**, 298 (1965); Phys. Rev. **154**, 1174 (1967).

[10] S. W. Cosper, J. Cerny, and R. G. Gatti, Phys. Rev. **154**, 1193 (1967).

[11] J. C. Watson, Phys. Rev. **121**, 230 (1961).

[12] H. E. Wegner, Bull. Am. Phys. Soc. **6**, 307 (1961).

[13] D. L. Horrocks, Phys. Rev. **134**, B1219 (1964).

III. EXPERIMENTAL RESULTS AND DISCUSSION

A. The Characteristics of the α Particles

In Figs. 2–4 we present the angular and energy distributions of the α particles in the LRA fission of Cf^{252}.

In Fig. 2, the total angular distribution of the α particles as a function of the angle θ_L between the α-particle counter and the direction of the light fragment is presented. Two curves are shown in this figure. The "uncorrected" curve shows the experimentally obtained angular distributions without corrections for the finite size of the detectors and the source. When these corrections are taken into account, the "corrected" curve is obtained. The finite-size corrections are discussed in detail in Appendix I. All other angular distributions shown in this paper have been corrected for the finite size of the detectors and source. The reason for presenting both curves in Fig. 2 is twofold: (1) to show that the peak position is virtually unchanged by applying the correction for finite detector and source size. This is due to the fact that the "uncorrected" curve is essentially symmetric with respect to the most probable angle. The same is true for the majority of the angular distributions which are presented in this paper. In other words the peak positions are essentially unaffected by the corrections and hence certain approximations used in the correction procedure (see Appendix I) are not expected to affect the peak position within our experimental accuracy. (2) The corrections do have a marked effect on the wings of the distribution, decreasing the FWHM (full width at half-maximum) by 25%, from 43.5° to 32.5°. It follows that because of the approximations used in the correction procedure the correct shape of the distributions is somewhat in doubt. This is particularly true for the outer wings of the distributions, where the series expansion used in the correction procedure does not converge rapidly and shows considerable variations as the next higher term is included. For this reason, the outer wings of the distribution cannot be trusted. For example, the corrected curve in Fig. 2 seems to flatten off at $\theta_L - 110°$ to a value slightly above the isotropic random-coincidence value (which is the minimum to be expected at any angle). This would seem to indicate that the true distribution goes almost to zero at approximately $\theta_L = 120°$. However, in view of the uncertainties involved this conclusion is probably not justified, although the true value is certainly quite small at these angles. Similarly some of the angular distributions to be shown below show curves which seem to approach or even cross the zero line. In view of the finite number of random events associated with all the distributions, the former possibility is not likely. The latter is obviously impossible. The ordinate of all angular distributions shown refers to the number of counts per unit *solid* angle (rather than geometrical angle). Hence the random coincidences and similar events provide a constant background on all curves.

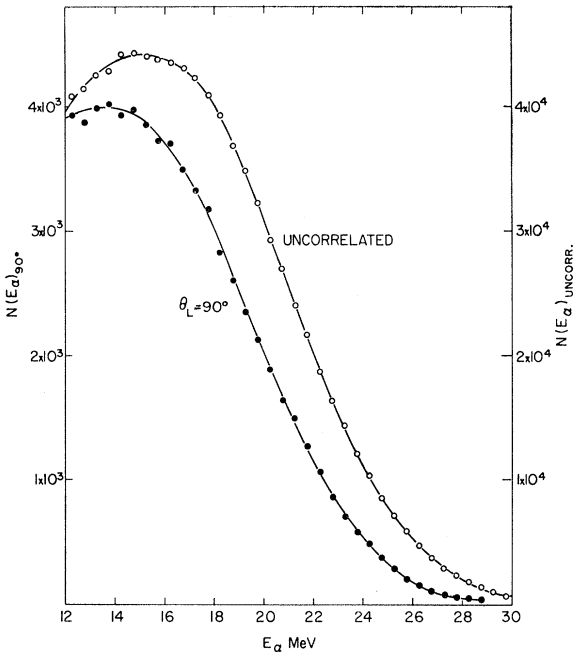

FIG. 3. The kinetic-energy distribution of the α particles measured at an angle $\theta_L = 90°$ and uncorrelated with the fission fragment direction.

The corrected angular distribution is approximately symmetric around a most probable value of 81° and it has a width (FWHM) of 32.5°. These characteristics are in reasonable agreement with the distribution obtained for Cf^{252} by Muga *et al.* with the aid of photographic emulsions.[14] There is even better agreement with the results of Perfilov and Solov'eva[15] for U^{235}, indicating that the angular distribution of the α particles in the LRA fission is essentially independent of the fissioning species and to some extent of the excitation energy. The work of Perfilov and Solov'eva was also done with the aid of nuclear emulsions. The agreement with the earlier work on U^{235} by Titterton[2], who also used emulsions, is somewhat less satisfactory.

Figure 3 shows the α-particle energy distribution obtained in coincidence with the two fission fragments at an angle of 90° between the α-particle counter and the fission-fragment counters. Also shown is the "uncorrelated" α-particle spectrum which is obtained when the α-particle spectrum is measured without a coincidence requirement (i.e., without regard to the angle with respect to the fission fragments). The α-particle threshold in this experiment was normally 10 MeV. Because of the greater sensitivity of the energy distribution to possible background from contamination, we show this distribution only for values greater than 12.0 MeV, where this background was completely negli-

[14] M. L. Muga, H. R. Bowman, and S. G. Thompson, Phys. Rev. **121**, 270 (1961).

[15] N. A. Perfilov and Z. L. Solov'eva, Zh. Eksperim. i. Teor. Fiz. **37**, 1157 (1959) [English transl.: Soviet Phys.—JETP **10**, 825 (1960)].

gible. (A background subtraction procedure was not considered to be justified in view of the exceedingly long counting time required for adequate statistics.) The corrections to the spectrum due to straggling in the absorber foil are completely negligible. The main characteristics of the 90° energy distribution are the maximum at 14 MeV and the half-maximum value at 20 MeV. In the uncorrelated α-particle spectrum, the maximum is shifted to 15 MeV and the half-maximum point is shifted to 21.5 MeV. The latter values are to be compared with the results of Watson,[11] Muga *et al.*,[14] and Nobles,[7] all of whom measured the α-particle energy distribution for Cf^{252}. Our results are in good agreement with the results of Watson and Nobles, except that the most probable value of the α-particle energy distribution obtained by these authors (mostly with rather poor statistics) is somewhat higher (16–17 MeV) than our value. Our results are in definite disagreement with the results of Muga *et al.*[14] who obtained the peak in the α-particle distribution at approximately 19 MeV. The reason for this discrepancy is not known.

Figure 4 shows the average value of the α-particle kinetic energy $\bar{E}_\alpha$ as measured in this experiment and the standard deviation σ_α of the α-particle energy distribution as function of the final angle θ_L of the α particle with respect to the light fragment. It should again be pointed out that both $\bar{E}_\alpha$ and σ_α were computed for α-particle energies *above* 10 MeV. Thus the true average value is smaller than the value shown in Fig. 4, whereas the true standard deviation (roughly the half-width) is larger than σ_α shown in Fig. 4. However, our

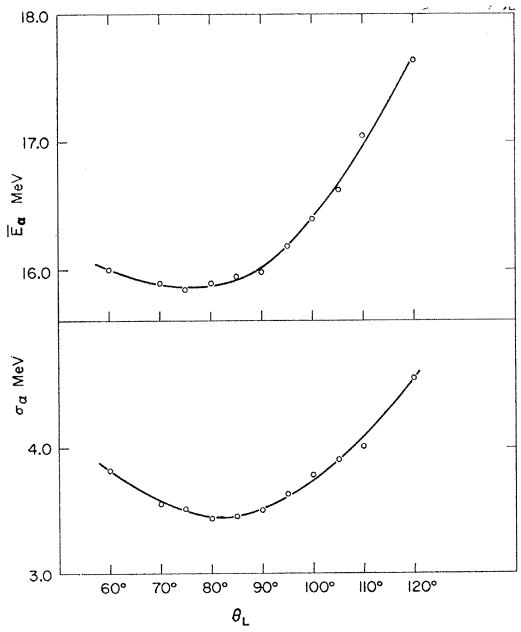

FIG. 4. The mean value $\bar{E}_\alpha$ and standard deviation σ_α of the α-particle kinetic-energy distribution as a function of the final angle θ_L. Only α particles of energy above 10.0 MeV were measured, and therefore $\bar{E}_\alpha$ and σ_α have only relative meaning.

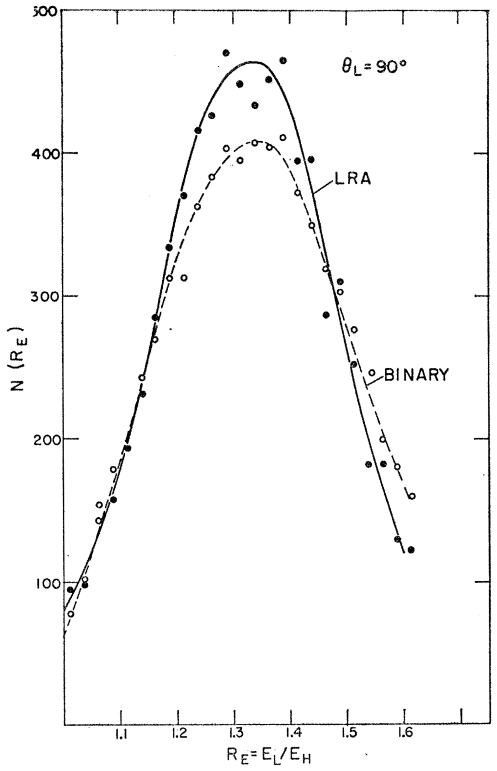

FIG. 5. The fission-fragment energy ratio distribution for LRA fission (θ_L=90°) and binary fission.

low-energy cutoff is not expected to have much effect on the shape of the curves in Fig. 4, and only the energy scale must be shifted. We see that both $\bar{E}_\alpha$ and σ_α reach a minimum at approximately the most probable angle. The angle θ_L=90° is near the most probable angle and therefore the mean value of the α-particle energy distribution measured at θ_L=90° (Fig. 3) is lower than the mean value at most of the other angles. The same is true for the most probable value of the energy distribution, and that is the reason that a lower value is obtained for the peak position of the 90° curve in Fig. 3, as compared to the uncorrelated α-particle distribution.

The two curves shown in Fig. 4 can be explained by the variation of the potential-energy surface around the nucleus at the moment of scission. This surface has a shallow minimum, the position of which depends on the mass ratio, and it rises steeply near the two fragments. This shape of the surface causes α particles which are emitted near the heavy fragment to be directed towards the light fragment (small θ_L) and *vice versa*. α particles emitted near the potential-energy minimum will have a final angle of $\theta_L \simeq 80°$ (the most probable angle). Hence the α particles with small final angles θ_L and very large θ_L which are emitted close to one of the fragments have a higher potential energy, and this fact is reflected in the higher average final energy, as seen in Fig. 4. The variation of σ_α with θ_L as seen in Fig. 4 can similarly

be explained by the variation of the potential-energy surface. Since the final angle of the α particle is to some extent also dependent on other variables (besides the point of emission) such as the initial energy and the initial angle, a given final angle corresponds to a *distribution* of emission points. Since the potential-energy surface changes more rapidly near the two fragments, it follows that α particles with very small or very large final angles correspond to a wider initial potential-energy distribution. This fact is reflected in the larger standard deviation of the final kinetic energy for the extreme angles, as seen in Fig. 4.

The belief that the α particles are emitted from the "neck" region between the two scissioning fission fragments has so far been based on the angular distribution of the α particles.[3] Figure 4 presents independent support for this assumption. It indicates that the α particle is emitted from the potential-energy valley between the two fragments. It is emitted from various points in this valley with different probability, as seen from Fig. 2.

If we assume that α particles with final angles near the most probable value (81°) are emitted near the potential-energy minimum, then the value of σ_α for this angle is to a first approximation the result of the initial *kinetic*-energy distribution. Hence an estimate of this initial distribution can be obtained from Fig. 4.

Our interpretation of Fig. 4 is based on the assumption that the final angle θ_L of the α particle is determined predominantly by the initial position (i.e., emission point) rather than the initial angle and energy. This assumption is supported by the trajectory calculations which are discussed in the following paper.[16] In that paper, we also give a quantitative estimate of the initial energy and angular distributions of the α particles which is based on Figs. 2–4.

B. The Characteristics of the Fission Fragments in LRA Fission and the Comparison with Binary Fission

In Figs. 5–7 we present some of the basic characteristics of the two fission fragments in LRA fission.

Figure 5 shows the energy-ratio distribution for LRA fission at $\theta_L=90°$ and for binary fission.

The energy ratio $R_E=E_L/E_H$ (where E_L is the kinetic energy of the light fragment, and E_H is the kinetic energy of the heavy fragment) is to a first approximation equal to the mass ratio m_H/m_L. This approximation neglects the effect of the evaporation of neutrons and of the recoil momentum of the α particle. The latter effect is negligible ($\approx 0.3\%$) for $\theta_L=90°$ (see Appendix II).

The scale of the ordinate of Fig. 5 pertains to the LRA-fission curve. The binary-fission curve (for which the statistics are much better) has been normalized to the same area (including values above $R_E=1.6$ which are not shown in Fig. 5). The reason for the comparatively poor statistics of the LRA curve is that the $N(R_E)$ curve is particularly sensitive to detector deterioration (which results in widening of the curve), and hence only the data of runs in which the detector deterioration was negligible are presented in Fig. 5. In all other results presented in this paper, rather wide energy ratio intervals were used, and hence there the detector deterioration problem was less critical. The essential features of Fig. 5 may be summarized as follows:

(1) The energy ratio distributions for LRA and binary fission are very similar.

(2) The most probable energy ratios are the same for the two processes within the statistical accuracy.

(3) The energy ratio distribution for LRA fission is slightly narrower as a result of the fact that energy ratios with $R_E>1.5$ are slightly less probable in LRA fission. A relative decrease for high mass ratios compared to those of binary fission is to be expected on general grounds, because of the lack of four nucleons in the combined mass of two fragments. Halpern[17] arrived at a similar conclusion by analyzing the experimental results of Schmitt *et al.*[18] for LRA fission of U^{235} induced by thermal neutrons.

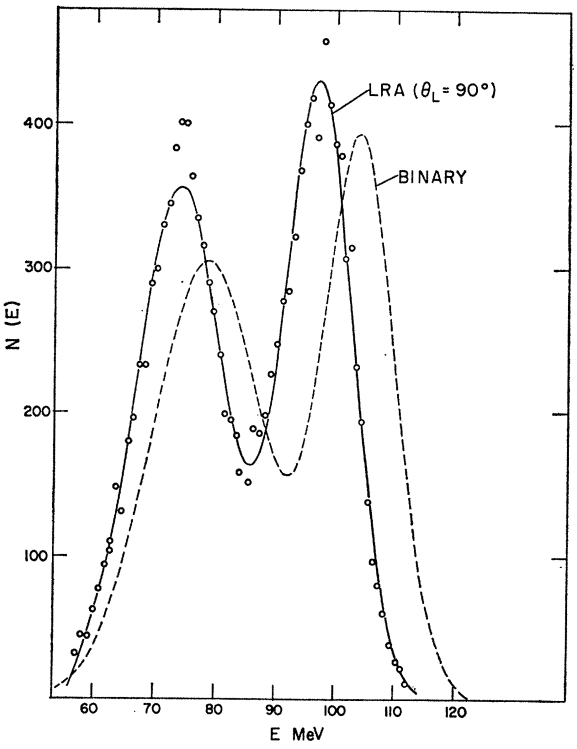

FIG. 6. The single-fragment energy distribution in LRA fission ($\theta_L=90°$) and binary fission.

[16] Y. Boneh, Z. Fraenkel, and Y. Nebenzahl, following paper Phys. Rev. **156**, 1305 (1967).

[17] I. Halpern, in *Symposium on the Physics and Chemistry of Fission* (International Atomic Energy Agency, Vienna, 1965), Vol. II, p. 369.

[18] H. W. Schmitt, J. H. Neiler, F. J. Walter, and A. Chetham-Strode, Phys. Rev. Letters **9**, 427 (1962).

TABLE I. Mean values $\bar{E}$ and standard deviations σ of the kinetic energy of the heavy and light fragments when fitted to two-Gaussian distributions. Results for two different weightings of the experimental data are given. Also shown are the areas A under the Gaussian curves. The measurements were made at $\theta_L=90°$. The errors are statistical only.

	LRA		Binary	
Weighting	1	Y^{-1}	1	Y^{-1}
$\bar{E}_H$ (MeV)	74.3 ±0.1	74.2 ±0.1	78.8 ±0.2	78.8 ±0.2
σ_H (MeV)	7.16±0.06	7.48±0.06	8.89±0.12	9.22±0.12
A_H	6965	7039	2758	2776
$\bar{E}_L$ (MeV)	97.3 ±0.1	97.2 ±0.1	104.1 ±0.1	104.1 ±0.1
σ_L (MeV)	5.75±0.05	5.66±0.05	6.22±0.09	5.89±0.09
A_L	6493	6370	2336	2239
A_H/A_L	1.07	1.11	1.18	1.24

We show in Fig. 6 the single-fragment energy distribution $N(E_S)$ for LRA fission at $\theta_L=90°$ and for binary fission. (It should be mentioned that the single-fragment energy distribution at any angle except $\theta_L=90°$ is distorted by the fact that the number of light fragments detected is not equal to the number of heavy fragments, as a result of the LRA angular distribution, which is shifted towards the light fragment. Thus if an angle $\theta_L\neq 90°$ is chosen, the single spectrum of the two fission-fragment detectors must be combined before a useful comparison with binary data can be made.) Similar results have been obtained by Dmitriev *et al.*[19,20] for U^{233}, U^{235}, and Pu^{239}.

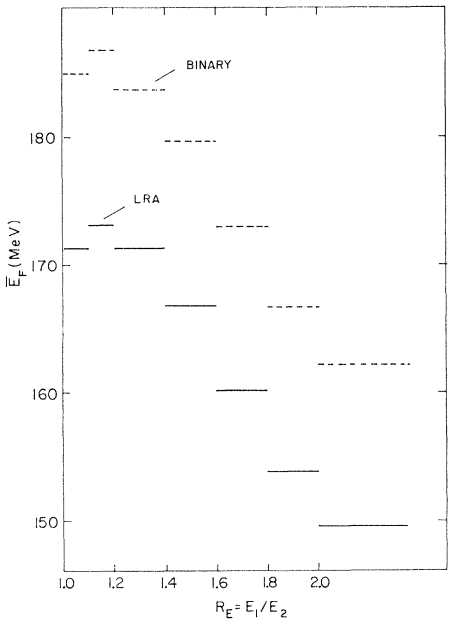

FIG. 7. The mean fission-fragment kinetic energy $\bar{E}_F$ in LRA fission ($\theta_L=90°$) and binary fission as a function of the fission-fragment energy ratio.

The experimental data were fitted with two Gaussian distributions with the aid of a modified version of the Los Alamos general least-squares fitting program.[21] The fitting procedure was done with both equal weighting and statistical y_i^{-1} weighting. The mean value, standard deviation, and area (i.e., number of counts) for each of the two Gaussian curves is shown in Table I. It is seen that the differences between the results of the two weighting procedures are very small. The fact that the areas under the two peaks are not exactly equal shows that the single-fragment energy distribution cannot be accurately described by two Gaussian distributions. This discrepancy is somewhat smaller for LRA fission than for binary fission and seems to be somewhat smaller for equal weighting. However, since statistical weighting is generally the more appropriate procedure, this weighting was used in Fig. 6. The binary-fission curve has been normalized to the same total area as the LRA-fission curve. The characteristics of Fig. 6 and Table I may be summarized in the following way:

(1) The two single-fragment energy distributions are similar in all their main features. However, the high- and low-energy peaks are narrower for LRA fission.

(2) The high-energy peak in LRA fission is shifted by approximately 7 MeV compared to binary fission, whereas the low-energy peak is shifted by only 4.5 MeV. As a result the total distribution is also narrower for LRA fission.

(3) The two peaks are more nearly equal (in width and height) for LRA fission ($\sigma_1/\sigma_2=1.32$, statistical weighting) than for binary fission ($\sigma_1/\sigma_2=1.57$).

In Fig. 7 we show the average total fission-fragment energy $\bar{E}_F$ ($E_F=E_L+E_H$) as a function of the energy ratio R_E for LRA fission and binary fission. Except for an energy shift of approximately 12 MeV, the two graphs are essentially identical. Both show a small dip of approximately 2 MeV near symmetric fission. Similar results have been obtained for LRA fission of U^{235} by Schmitt *et al.*[18] Our values for binary fission are in excellent agreement with the results of Whetstone[22] except

[19] V. N. Dmitriev, L. V. Drapchinskii, K. A. Petrzhak, and Yu. F. Romanov, Zh. Eksperim. i. Teor. Fiz. **39**, 556 (1960) [English transl.: Soviet Phys.—JETP **12**, 390 (1961)].

[20] V. N. Dmitriev, L. V. Drapchinskii, K. A. Petrzhak, and Yu. F. Romanov, At. Energ. (USSR) **14**, 574 (1963) [English transl.: Soviet J. At. Energy **14**, 599 (1964)].

[21] R. H. Moore and R. K. Zeigler, Los Alamos Scientific Laboratory Report No. LA 2367, 1959 (unpublished).

[22] S. L. Whetstone, Jr., Phys. Rev. **131**, 1232 (1963).

for a shift of approximately 2 MeV. This shift is the result of the discrepancy of approximately 2 MeV between the value of $\bar{E}_F$ as obtained by Fraser *et al.*[8] (which we use for energy calibrations) and the results of Whetstone. (This discrepancy has recently been attributed[23] to the effects of scattering from the walls of the flight tubes in the experiment of Fraser *et al.*[8])

The differences between the binary and LRA curves in Figs. 5 and 6 are perhaps best discussed in terms of a third diagram, namely, in E_1 versus E_2 contour diagram (E_1 and E_2 are the kinetic energies of the two fragments). This diagram contains all the information shown in Figs. 5–7 and the latter figures may be obtained from the E_1 versus E_2 contour diagram by an appropriate integration procedure. For lack of adequate statistics (which must be extremely good in order to show small differences in a contour diagram) for showing the actual experimental results, we show instead a somewhat idealized diagram of this type in Fig. 8. The four points denote the low- and high-energy peaks of the two-dimensional energy distributions for LRA and binary fission. They were assumed to be identical with the average values $\bar{E}_1$ and $\bar{E}_2$ of the single-fragment energy distributions (Table I). The solid ellipses denote the contours of half-maximum values for LRA fission, whereas the dashed ellipses denote those of binary fission. The major and minor axes of the ellipses are equal to the standard deviations σ_1 and σ_2, respectively, of the single-fragment energy distributions (Table I). The major axes of the ellipses were assumed to be parallel to the E_1=constant and E_2=constant lines. None of the above assumptions is strictly correct. However, the errors involved do not affect our qualitative arguments: It is seen that the peak values for LRA fission are slightly shifted towards the $R=1$ line. Also the eccentricity of the LRA ellipses is somewhat smaller. The combined effect of these two small differences is that $R\gg1$ is less probable in LRA fission than in binary fission, whereas the R distribution is approximately the same for $R<1.3$. The smaller eccentricity is reflected in the more nearly equal shape of the low- and high-energy peaks in the LRA single-fragment energy distribution (Fig. 6).

The most important characteristic of Figs. 5–7 is the similarity of the graphs for LRA and binary fission. *The great similarity of the curves of $N(R_E)$, $N(E_S)$, and $\bar{E}_F(R_E)$ for LRA and binary fission makes it highly improbable that the two processes differ in any substantial aspect up to the moment of scission.*

We have not tried to transform the single-fragment *energy* distribution (Fig. 6) into a single-fragment *mass* distribution. The reason is that to perform this transformation we must correct for two effects: (a) the number and kinetic energy of the neutrons emitted in LRA fission as a function of the fragment mass number; (b) the effect of the recoil momentum due to the α particle. The correction for the α-particle recoil is quite small for $\theta_L=90°$ and can be evaluated with sufficient accuracy (see Appendix II). On the other hand, the correction for neutron emission can so far only be estimated. The uncertainties connected with this estimate are large enough to affect seriously the comparison of the single mass yield in LRA and binary fission, since the differences involved are relatively small.

[23] J. S. Fraser, in *Symposium on the Physics and Chemistry of Fission* (International Atomic Energy Agency, Vienna, 1965), Vol. I, p. 541.

C. The Angular Distribution of the α Particles as a Function of the α-Particle Kinetic Energy

In Fig. 9(a) we show the angular distribution of the α particles for four α-particle kinetic-energy intervals. (The curves for the energy intervals 13–15 MeV and 15–17 MeV are very similar to curves 1 and 2 and are therefore omitted.) The most striking feature of this family of curves is the fact that the angular distribution is almost energy-independent up to an energy of 19 MeV, and the angular distribution of all α particles above 23 MeV is almost isotropic. Results similar to Fig. 9(a) have been obtained for U^{235} by Perfilov and Solov'eva[15] with the aid of nuclear emulsions. However, if the high-energy part of the α-particle angular distribution is analyzed in greater detail, we find that the transition from a highly peaked distribution to an almost isotropic one is gradual, as is seen from the three curves for the energy interval $19\leq E_\alpha<25$ MeV [curves 1–3 of Fig. 9(b)], and that the "isotropic" distribution for $E_\alpha>23$ MeV which is seen in Fig. 9(a) is the result of the superposition of a convex (peaked) distribution for the interval $23\leq E_\alpha<25$ MeV and a concave distribution above 25 MeV. The characteristics of Figs. 9(a) and 9(b) may be summarized as follows: (1) Below $E_\alpha\simeq20$ MeV the angular distribution is almost energy-independent. (2) In the energy region of 20 MeV$\leq E_\alpha<25$ MeV the angular distribution widens until it becomes essentially isotropic. (3) Above $E_\alpha\simeq25$ MeV

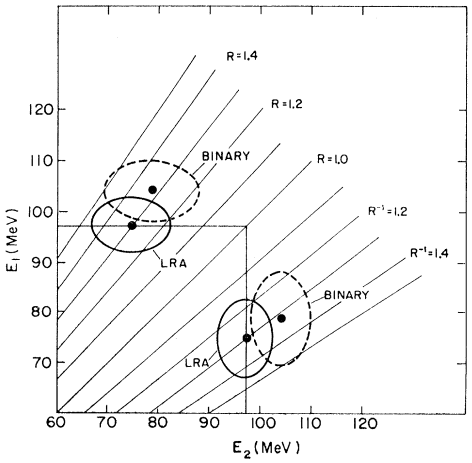

FIG. 8. Schematic E_1-versus-E_2 plot for LRA fission ($\theta_L=90°$) and binary fission.

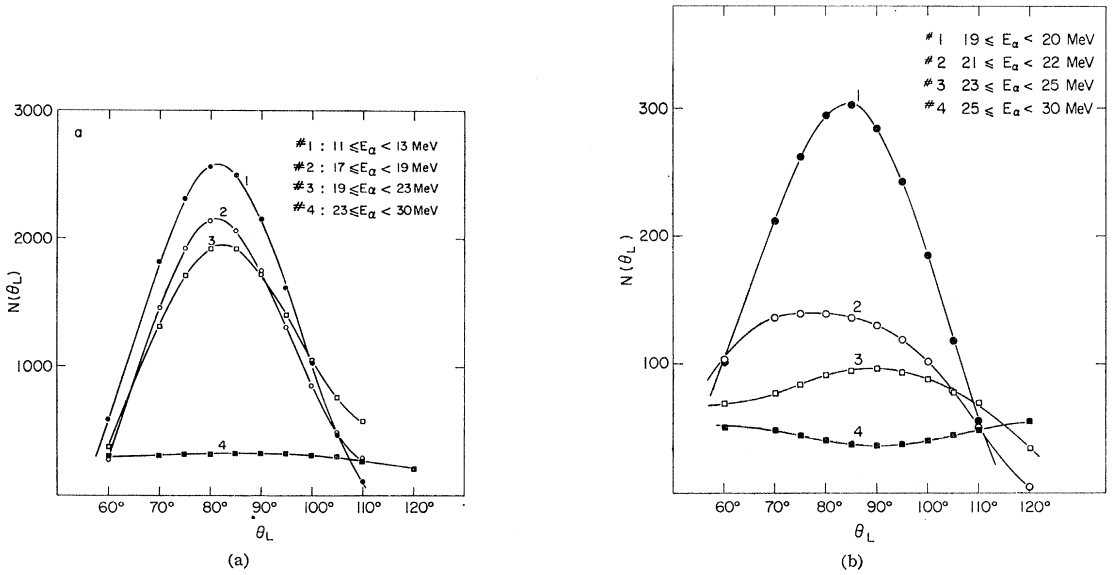

FIG. 9. The α-particle angular distribution for four intervals of the α-particle kinetic energy (a) in the region 11 MeV $\leq E_\alpha < 30$ MeV; (b) in the region 19 MeV $\leq E_\alpha < 30$ MeV.

the angular distribution has a concave shape with the minimum near the most probable angle for α particles with energy below 25 MeV.

Our interpretation of Figs. 9(a) and 9(b) assumes that in the energy region below $E_\alpha \simeq 20$ MeV the final energy distribution of the α particles is determined predominantly by the initial *kinetic*-energy distribution at the moment of emission. Since the final angle of the α particle is almost independent of its initial kinetic energy, the angular distribution is almost energy-independent. However, very high final kinetic energies are predominantly the result of a high initial *potential* energy, since very high initial kinetic energies are very unlikely if the initial kinetic-energy distribution has a Maxwellian or Gaussian shape. [The parameters of these distributions may be obtained from $N(E_\alpha)$, Fig. 3.] The α particles which have high initial potential energies are those which are emitted very near to one of the fragments, and the final direction of these α particles is close to the direction of the other fragment, e.g., an α particle emitted close to the heavy fragment will have a small final angle θ_L. The effect of the initial potential energy becomes important above 20 MeV, and as a result the angular distribution widens. A final energy above 25 MeV is likely only if the α particle is emitted near one of the fragments and the slope of the angular distribution changes from convex to concave.

The above arguments are supported by the trajectory calculations, and the experimental results give further support to the assertion that the final angle of the α particle is mainly determined by its initial position (i.e., the point of emission) rather than by its initial kinetic energy or initial angle of emission.

D. The Angular Distribution of the α Particles as a Function of the Fission-Fragment Mass Ratio: Detailed Analysis

In a previous paper[5] we have shown the angular distribution of the α particles for seven intervals of the fission fragment energy ratio R_E. The most striking characteristic of this family of curves is the shift of the peak of the distribution from $\theta_L(\text{peak}) = 70°$ for the interval $1.0 \leq R_E < 1.1$ to $\theta_L(\text{peak}) = 100°$ for the interval $2.0 \leq R_E < 10.0$.

We offered there two essentially equivalent explanations for this shift. The first explanation was based on a model first proposed by Vladimirski[24] and in somewhat different form by Whetstone.[25] The Whetstone model assumes the shape of the nucleus at the point of scission to resemble an asymmetric "dumbell," i.e., two more or less spherical parts of unequal size connected by a thin neck. This shape is assumed to be independent of the final mass distribution. The final mass ratio is determined by the point along the neck at which the scission occurs. The most probable mass ratio is obtained when scission occurs in the middle of the neck; symmetric fission, when the scission point is near to the larger fragment; and very asymmetric fission, when the scission point is near the smaller fragment. Such a simplified model would also explain the shift in the most probable angle of the α particles with the energy ratio R_E if we assume the α particle to be emitted at the point of scission (see below).

[24] V. V. Vladimirski, Zh. Eksperim. i. Teor. Fiz. **32**, 822 (1957) [English transl.: Soviet Phys.—JETP **5**, 673 (1957)].
[25] S. L. Whetstone, Jr., Phys. Rev. **114**, 581 (1959).

The second explanation was based on a somewhat more sophisticated version of the Whetstone picture. This version assumes the scission configuration for the most probable mass ratio to consist of two approximately equally deformed fragments of unequal size which are connected at the point of their maximal deformation. This point is also the ultimate scission point. The scission configuration for almost symmetric fission is assumed to consist of an almost spherical heavy fragment and a highly deformed light fragment. For very asymmetric fission the scission configuration is assumed to consist of an almost spherical light fragment and a highly deformed heavy fragment. The reason for the unequal deformation for $R\simeq 1$ and $R\gg 1$ is believed to be the closed nuclear shells which occur for these mass ratios for the heavy and light fragment, respectively. The primary purpose of these models was to explain the variation of the average number of fission neutrons with fragment mass, $\bar{\nu}(A)$, in binary fission. However, they are also capable of explaining qualitatively the shift of the most probable angle of the α particle with R_E in LRA fission.

A quite different explanation of the shift of the angular distribution with the energy ratio is based on purely kinematical arguments: If the α particle is emitted close to the heavy fragment it will be accelerated towards the light fragment. It will also give the heavy fragment a larger recoil momentum than the light fragment and in this way increase the energy of the heavy fragment, with the result that the energy ratio R_E of the two fission fragments decreases. Similarly, an α particle emitted near the light fragment will be accelerated towards the heavy fragment and at the same time will cause an increase in the energy ratio R_E. Thus a small value of θ_L is associated with a smaller value of R_E and vice versa. In a similar fashion, the initial angle of emission of the α particle affects the final angle θ_L and the energy ratio R_E. A quantitative discussion of this kinematic effect is presented in Appendix II.

Figure 10 shows the angular distribution of the α particle for four intervals of the energy ratio R_E corrected for the alpha-particle recoil, as discussed in Appendix II. Figure 10 shows, therefore, the angular distribution as a function of the mass ratio R, except for corrections due to neutron emission. The angular distributions shown in Figs. 11 and 12 below have also been corrected for the effect of the α-particle recoil on the energy ratio. These distributions can therefore be directly compared with the results of the trajectory calculations in the following paper.[16]

TABLE II. Mean value $\bar{E}_\alpha$ (averaged over solid angle between $\theta_L=60°$ and $\theta_L=120°$) of the α-particle kinetic energy for seven intervals of the fission-fragment mass ratio R. Only α particles of energy above 10.0 MeV were measured and therefore the values of $\bar{E}_\alpha$ have only relative meaning. The stated errors are statistical.

R interval	$\bar{E}_\alpha$
$1.0\leq R< 1.0$	16.26±0.04
$1.1\leq R< 1.2$	16.24±0.03
$1.2\leq R< 1.4$	16.07±0.02
$1.4< R< 1.6$	16.04±0.02
$1.6< R< 1.8$	16.06±0.05
$1.8< R< 2.0$	16.02±0.10
$2.0< R<10.0$	16.00±0.15

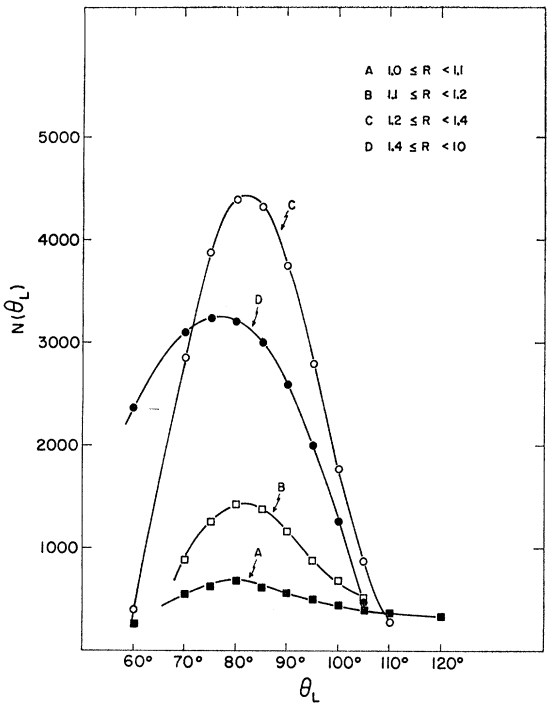

FIG. 10. The α-particle angular distribution for four intervals of the fission-fragment mass ratio R.

The comparison of the angular distribution as a function of the mass ratio R (Fig. 10) with the angular distribution as a function of the energy ratio R_E presented in the previous publication[5] shows that the α-particle recoil indeed causes a substantial change in the angular distribution. Figure 10 shows a small shift towards larger θ_L as R increases from $R=1.0$ to $R=1.2$, but for larger values of R the trend is reversed, and the most probable angle decreases with increasing R. The peculiar behavior of the most probable angle as a function of R again indicates a shift in the most probable scission point towards the light fragment as the mass ratio increases. This is discussed in greater detail in the following paper. There it is concluded on the basis of Fig. 10 that the most probable scission point shifts by approximately 5×10^{-13} cm towards the light fragment as the mass ratio increases from $R=1.0$ to $R=2.0$. This shift is much larger than that expected on the basis of electrostatic considerations (change in the position of the saddle point in the potential-energy surface). Thus our earlier conclusion with respect to the shift of the scission point, which was based on the angular distribution as a function of the energy ratio, is confirmed by Fig. 10.

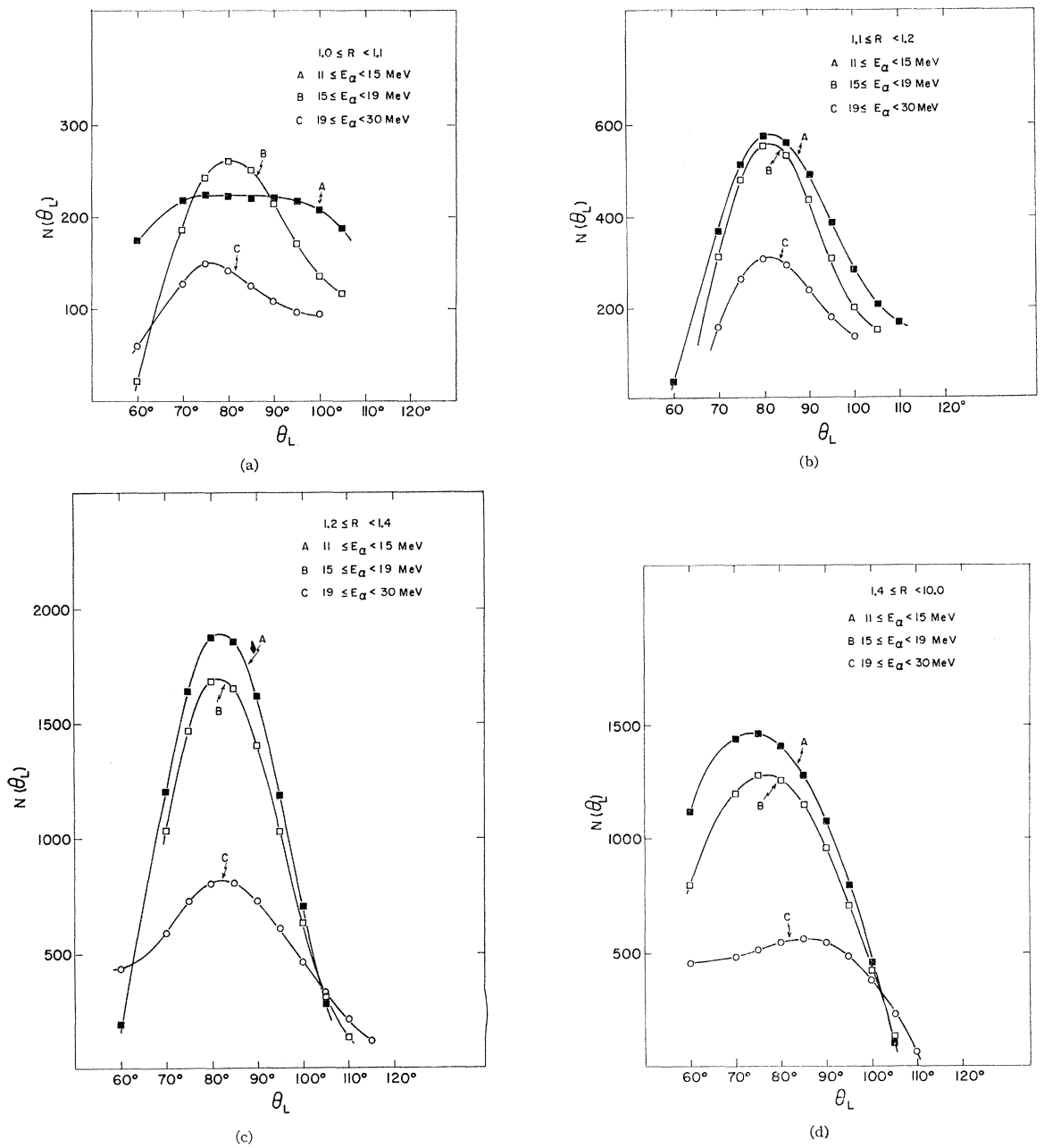

FIG. 11. The α-particle angular distribution for three intervals of the α-particle kinetic energy, subject to the condition that the fission-fragment mass ratio is (a) in the interval $1.0 \leq R < 1.1$; (b) in the interval $1.1 \leq R < 1.2$; (c) in the interval $1.2 \leq R < 1.4$; (d) in the interval $1.4 \leq R < 10.0$.

Table II shows the average α-particle energy for seven mass-ratio intervals. The data have been corrected for the α-particle recoil. Table II was obtained by averaging over the solid angle between $\theta_L = 60°$ and $\theta_L = 120°$ (i.e., the range of the experimental measurement). The values of $\bar{E}_\alpha$ are of relative significance only because they pertain to α particles with energy above $E_\alpha = 10$ MeV.

In Figs. 11(a)–11(d) we show the angular distribution of the α particles as a function of E_α for four intervals of the fission-fragment mass ratio R. [As mentioned above, the data presented in Figs. 11 as well as those of Figs. 12 below have been corrected for the α-particle recoil. However, in view of the uncertainties in this correction (see Appendix II) these distributions were also calculated without this correction. All the characteristics of Figs. 11 and 12 to be discussed in this section are also present in the "uncorrected" distributions. They are therefore believed to be unaffected by the accuracy of our correction procedure.] We see that

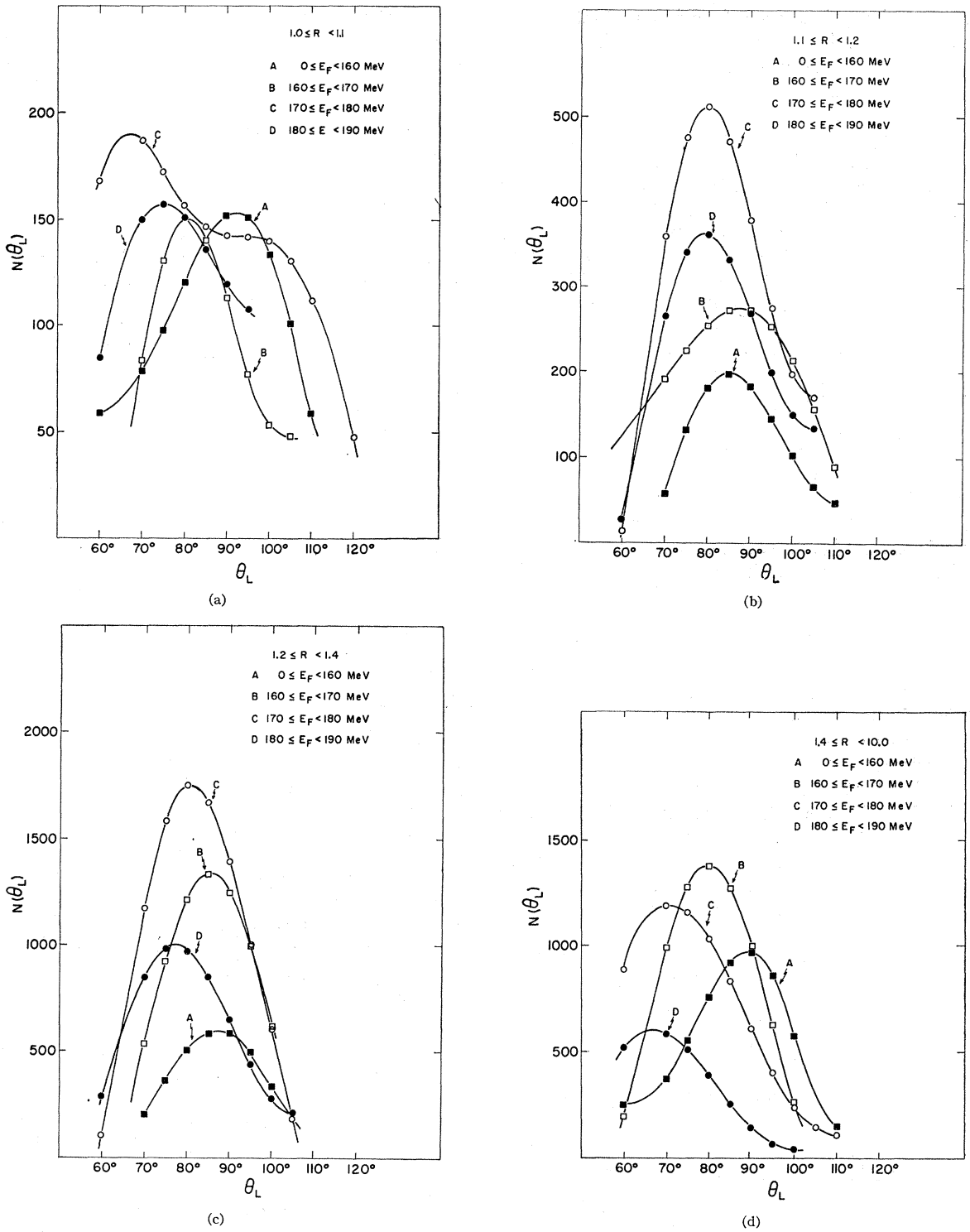

FIG. 12. The α-particle angular distribution for four intervals of the fission-fragment kinetic energy E_F, subject to the condition that the fission-fragment mass ratio is (a) in the interval $1.0 \leq R < 1.1$; (b) in the interval $1.1 \leq R < 1.2$; (c) in the interval $1.2 \leq R < 1.4$; (d) in the interval $1.4 \leq R < 10.0$.

for fission-fragment mass ratios close to $R=1$ the peak of the distribution shifts to lower θ_L as E_α increases, whereas for $R \gg 1$ the peak shifts to higher θ_L with increasing E_α. The shift as a function of E_α for a given R and for mass ratios close to $R=1$ and $R \gg 1$ can be explained as the result of small variations in the position

of the emission point. Even if we assume that a given mass ratio determines the position of the scission point, there must obviously be a finite variation of this position around the most probable point. For $R=1$ and $R\gg1$, the most probable points are assumed to be near one of the fragments. For these mass ratios even a small variation in the position of the point of emission will cause an appreciable change in both the final energy and final angle of the α particle. The closer the emission point to the fragment, the higher the final energy and the smaller the α-particle final angle with respect to the other fragment. This is a result of the rapid change of the initial potential energy with the position of the α particle near one of the fragments. If the emission point is in the center and not near either fragment (intermediate R values), the potential energy does not change rapidly as a function of position and hence no such effect is expected.

In Figs. 12 we show the angular distribution as a function of the fragment kinetic energy E_F for four regions of the mass ratio R. The graphs show a shift of the peaks of the angular distributions with the fragment kinetic energy. However, this shift is not the same for the various mass-ratio intervals. Thus in Fig. 12(a) there is a shift of the peak towards higher values of θ_L with increasing E_F (curve D as compared to curve C). For the mass-ratio interval $1.1\leq R\leq1.2$ [Fig. 12(b)] there is almost no shift of the peaks as a function of E_F; the shift is somewhat larger in Fig. 12(c) ($1.2\leq R<1.4$), and is quite considerable for curves C and D of Fig. 12(d) ($1.4\leq R<10$).

In order to interpret Fig. 12 we shall make the assumption that there exists a strong (negative) correlation between the total fragment *excitation energy* E^* and the total fragment *kinetic energy* E_F. This assumption is based on the fact that the total energy for a given mass ratio must be conserved and an increase in the fission-fragment kinetic energy must come at the expense of a decrease in their excitation energy and the kinetic energy E_α of the α particle. Since the variations in E_α are small compared to the variations in the fragment kinetic energy E_F, it follows that an increase in E_F must come predominantly at the expense of the excitation energy E^*. This is the case in binary fission,[26] and we assume the same to be true for LRA fission.

We have said that the variation of the α-particle angular distribution as a function of mass ratio may be interpreted in terms of the two "models" for the scission configuration in binary fission. One is the Whetstone picture[25] which assumes this configuration to have a shape of an "asymmetric dumbell" which is independent of the final mass ratio. If we accept this picture, a decrease in the final kinetic energy of the two fission fragments (or equivalently an increase in their excitation energy) would presumably result in a larger elongation of the neck connecting the two fragments, and no other changes in the scission configuration are to be expected. In LRA fission such an elongation would result at most in some change in the width of the α-particle angular distribution, but no change in the position of the peak of the distribution is to be expected. This is in disagreement with Fig. 12. These curves show a definite shift of the peak as a function of E_F, although this shift is small for some mass ratios. We therefore conclude that the Whetstone picture in its most naive version is not supported by our experimental results.

The second model explains the variation of the angular distribution with the mass ratio as a result of differing deformation of the fragments. It assumes that the lightest fragments in both the light and the heavy fragment groups normally have very little deformation energy. The amount of deformation energy increases with the fragment mass, and the heaviest fragments in the two fragment groups are normally highly deformed. We may now ask how differing amounts of total excitation energy E^* will affect the nuclear configuration at scission according to this model. For mass ratios close to $R=1$ the light fragment is normally highly deformed, whereas the heavy fragment is almost spherical. If the excitation energy E^* is decreased, this will cause the light fragment to be less deformed, whereas the heavy fragment will not be affected. This trend will continue as E^* is decreased until both fragments are almost spherical *and the configuration of the nucleus will be symmetric*. If, on the other hand, the excitation energy is increased above its average value, we may finally start to deform the heavy fragment as well (since the light fragment is already highly deformed), and we again approach a symmetrical configuration of the nucleus, this time with both fragments highly deformed. In LRA fission, we may therefore expect that for energy ratios close to *$R=1$ the peak of the α-particle angular distribution will shift towards $\theta_L=90°$ (symmetric nuclear configuration) for both very high and very low fragment kinetic energies*. This is exactly what is seen in Fig. 12(a). If curve A is indeed indicative of a symmetric nuclear configuration for very low kinetic energies E_F (i.e., very high E^*), this should also be evident in the number of neutrons emitted from the two fragments, which should be roughly equal. Past investigations have shown that the difference between the number of neutrons emitted from the two fragments becomes smaller as the kinetic energy decreases.[26] However, this specific point has not been the subject of a detailed investigation so far.

We shall now examine the effect of the excitation energy on nuclear scission configuration for other mass ratios. For intermediate values of R, our second model assumes approximately equal deformation energies for the two fragments. As the total excitation energy is changed, this will affect both fragments, and to a first approximation little change of the peak position in LRA fission is expected. This again is in agreement with the experimental results as seen in Fig. 12(b). For

[26] H. R. Bowman, J. C. D. Milton, S. G. Thompson, and W. J. Swiatecki, Phys. Rev. **129**, 2133 (1963).

higher mass ratios most of the excitation energy is concentrated in the heavy fragment. As the excitation is decreased, this fragment becomes more spherical, and the point of scission moves closer to the center of the heavy fragment. As a result the peak of the α-particle distribution is expected to shift to lower θ_L. This is seen in Fig. 12(d) and to some extent already in Fig. 12(c). For very high excitation energy E^* (i.e., for very low E_F), we would expect a reversal of the trend shown in Fig. 12(d), and the peak should move again towards lower values of θ_L as the light fragment also becomes deformed and the over-all nuclear configuration becomes more asymmetric. A possible reason for the fact that the shift in Fig. 12(d) does not reverse at low values of E_F may be the difference in the rigidity of the two fragments, which may well be higher for very asymmetric mass ratios [Fig. 12(d)] than for mass ratios close to $R=1$. Hence the increase in excitation energy (above the average value) which is needed to deform the closed-shell nucleus may be much higher for large mass ratios than for mass ratios close to $R=1$. Our interpretation of Figs. 12 cannot be fully trusted until this question is elucidated and the shift of the angular distribution towards higher values of θ_L indicated in Fig. 12(a), curve D, is established with better statistics.

Figures 12 show the angular distribution as a function of the fragment energy E_F for four intervals of the fragment mass ratio R. For sake of completeness we show in Fig. 13 this distribution when summed over all values of R. Curve E of Fig. 13 seems to include a substantial isotropic background. The possibility that this background is due to random coincidences or reactions other than LRA fission is discussed in Appendix III.

E. The Correlation between the Total Fragment Kinetic Energy E_F and the α-Particle Energy E_α

In this section we present experimental data which yield information on the correlation between the fragment kinetic energy E_F and the α-particle energy E_α. As will be discussed below, the correlation between these two qualities has bearing on the dynamics of the scission process.

We show in Fig. 14 the α-particle angular distribution as a function of the fragment kinetic energy E_F for four intervals of the α-particle energy E_α. Three features are evident (in addition to the shift to lower values of θ_L for increasing values of E_F which was already discussed in the preceding section): (1) A low α-particle energy E_α (10 MeV$\leq E_\alpha <$11 MeV) is associated with higher fragment energies E_F [among the curves of Fig. 14(a), curve C has largest peak] whereas a high α-particle energy (19 MeV$< E_\alpha$) is associated with lower fragment energies [among the curves of Fig. 14(d), curve B has the largest peak]. (2) The peak positions are independent of the α-particle energy. (3) Up to an

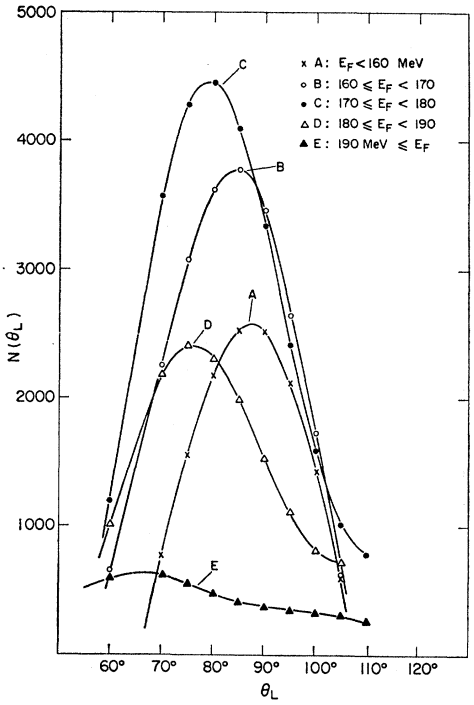

FIG. 13. The α-particle angular distribution for five intervals of the fission-fragment kinetic energy E_F.

energy of 19 MeV [Figs. 14(a)–14(c)], the width of the distributions does not vary with E_α.

The correlation between E_F and E_α is presented in a more quantitative form in Fig. 15. In this figure we show the mean value of the fragment energy $\bar{E}_F$ as a function of the α-particle energy E_α at a final angle $\theta_L=90°$. The absolute experimental error in the measurement of $\bar{E}_F$ may be as high as 0.5 MeV; however, this error is common to all values of $\bar{E}_F$. The relative experimental error is believed to be negligible. The measurements of Schmitt *et al.*[18] also yield information on the correlation between E_F and E_α. Their results seem to be in good agreement with our values. (Their results were presented in a different form and hence a direct comparison cannot be made.) On the other hand, Solov'eva and Filov[27] find a stronger correlation than shown in Fig. 15.

In discussing the angular distribution as a function of E_α (Fig. 9) we concluded, from the fact that up to an energy of $E_\alpha=19$ MeV both the position and the width of the angular distribution are independent of E_α, that the α-particle energy distribution up to an energy of $E_\alpha=19$ MeV is primarily caused by the initial kinetic-energy distribution of the α particles at the point of emission (rather than the variation of the initial potential energy). Figures 14(a)–14(c) show that this conclusion is quite independent of the fragment energy E_F.

[27] Z. I. Solov'eva and R. A. Filov, Zh. Eksperim. i. Teor. Fiz. 43, 1146 (1962) [English transl.: Soviet Phys.—JETP 16, 809 (1963)].

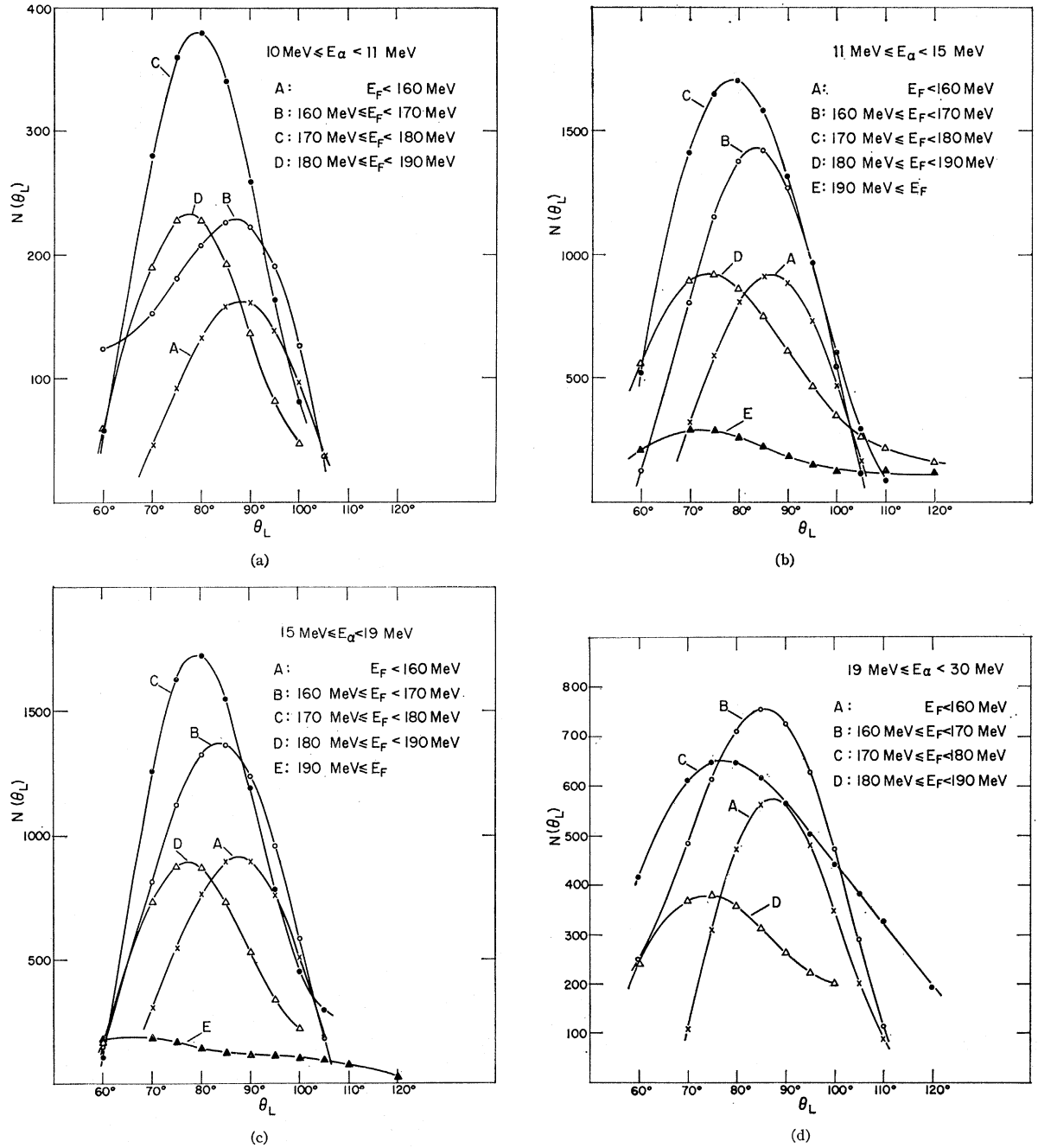

FIG. 14. The α-particle angular distribution for four intervals of the fission-fragment kinetic energy E_F, subject to the condition that the α-particle energy is (a) in the interval 10 MeV$\leq E_\alpha <$11 MeV; (b) in the interval 11 MeV$\leq E_\alpha <$15 MeV; (c) in the interval 15 MeV$\leq E_\alpha <$19 MeV; (d) greater than E_α=19 MeV.

In the following arguments we shall confine ourselves to the correlation between E_F and E_α for α-particle energies below E_α=19 MeV. For this region we shall make the following two assumptions: (a) The initial potential energy of the α particles is constant and the final kinetic-energy distribution is entirely due to the initial kinetic-energy distribution. (b) The average initial energy of the two fission fragments at scission is independent of the initial kinetic energy of the α particles. It follows that an increase in the α-particle kinetic energy E_α must be compensated to some extent by a decrease in the final fission fragment energy E_F. *However, the degree of correlation between E_α and E_F is critically dependent on the starting conditions at the moment of scission.* Thus if the kinetic energy of the three particles at scission is very small, any increase in

the α-particle energy must be compensated by a decrease of equal size in the fragment kinetic energy (i.e., the correlation coefficient is $r=-1$). If, however, the three particles have already acquired an appreciable part of their final kinetic energy at the moment of scission (and if up to this moment the kinetic energy of the fission fragments is not correlated to the kinetic energy of the α particle), then the amount of the observed correlation will be quite small. [Actually, the situation is somewhat more complicated, since there is an initial variation of the fission-fragment kinetic energy which is compensated (as in binary fission) by a similar change in the excitation energy of the fragments. However, if this initial distribution is uncorrelated with the initial kinetic energy of the α particle, our arguments are still valid with respect to the correlation between E_α and $\bar{E}_F$, the mean value of the fragment kinetic energy.] Halpern[6] has suggested that the fission fragments move at the moment of scission with an appreciable fraction of their final kinetic energy. The results shown in Fig. 15 support this view. These conclusions are in contradiction with the assumptions of the statistical model[28] which assumes very small (less than 0.5 MeV) fragment kinetic energies at scission. This subject is discussed in greater detail in the following paper.[16]

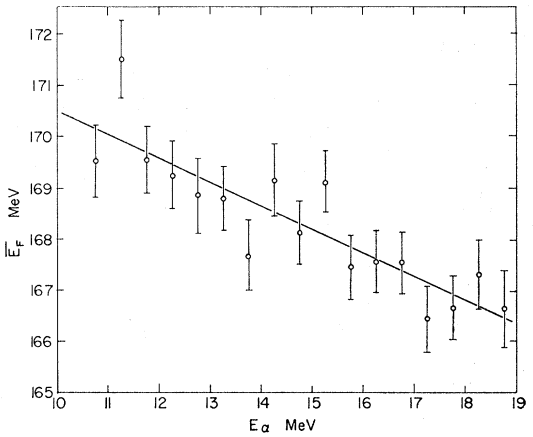

FIG. 15. The mean fragment kinetic energy $\bar{E}_F$ as a function of the α-particle kinetic energy E_α.

IV. CONCLUSIONS

In this section we summarize our conclusions with respect to the LRA-fission process, as well as those results which we believe to hold for binary fission as well.

(1) The most important conclusion with respect to LRA fission is that this process is very similar in all its aspects (except for the α-particle emission) to the binary-fission process. The most striking evidence for this conclusion is the great similarity of the fission-fragment energy-ratio distribution for the two processes (Fig. 5), and the similarity of the single-fragment energy distributions (Fig. 6) and of the total energy distributions as a function of the energy ratio (Fig. 7).

(2) The variation of the average kinetic energy of the α particle $\bar{E}_\alpha$ as a function of the angle θ_L indicates that the α particle is emitted from the potential minimum between the two fission fragments. This result may therefore be regarded as an additional support for the assumption that the α particle is emitted from the "neck" connecting the two fragments.[3]

(3) In this paper, as well as in a previous publication,[5] we have presented independent evidence for the conclusions of Terrell,[4] Vandenbosch,[29] and Fong[30] regarding the shape of the scissioning nucleus. So far these conclusions were based only on the observed variation of the average number of emitted neutrons as a function of the fragment mass A.

However, our results based on the angular distribution in LRA fission can be related to the shape of the scissioning nucleus only if we *assume that the α particles are emitted at the scission point or within a distance of order of 1 fermi from this point and very close to the moment of scission*, before the two fragments are widely separated (within 10^{-21} sec from the moment of scission). In fact, if we assume that the α particles are "evaporated" from one of the fragments after the two fragments are well separated, then our results are at variance with the results obtained from neutron studies, since on this assumption we would conclude from our results that the α particles are evaporated from the fragments of *lowest* excitation (the heavy fragment for $R\simeq 1$ and the light fragment for $R>\geq 1$). This possibility is very unlikely. We may thus interpret the results shown in Figs. 10–12 as substantial evidence that *the α particles in LRA fission are emitted very close to the point of scission and less than 10^{-21} sec from the moment of scission.*

Our conclusions regarding the similarity of LRA and binary fission and the proximity of scission and α-particle emission are the basis for using the LRA fission process as a tool for the investigation of the configuration of the nucleus at the point of scission in binary fission.

(4) The small amount of correlation between the mean fragment energy $\bar{E}_F$ and the α-particle energy E_α supports the view that at the moment of scission the fission fragments already move with an appreciable fraction of their final velocity. Additional support for this assumption comes from the trajectory calculations which are discussed in the following paper.

While the above-mentioned characteristics provide evidence for a large degree of similarity between the two fission processes up to the moment of scission, it has been pointed out by Halpern[6] that the scission configuration in LRA fission must be more stretched out than the average scission configuration in binary fission.

[28] P. Fong, Phys. Rev. **102**, 434 (1956).
[29] R. Vandenbosch, Nucl. Phys. **46**, 129 (1963).
[30] P. Fong, Phys. Rev. Letters **11**, 375 (1963).

This statement is based on two arguments: (a) The excitation energy in the average binary-fission process is insufficient for emitting an α particle from the neck. (b) The fact that the average total kinetic energy in LRA fission is only by 3 MeV higher (for Cf^{252}) than the average energy in binary fission, whereas the difference in kinetic energy should be considerably higher if the two scission configurations are identical.

A more stretched-out configuration at the scission point in LRA fission would be associated with a higher than average excitation energy, which is required for the emission of the LRA particle and also would result in a lower total kinetic energy of the three fragments.

We wish to examine briefly the two arguments. Let us assume that the scission configuration for both binary and LRA fission may be approximated by three point charges: the two fission fragments 1 and 2 and the α particle (point 3). We assume that the two fission fragments are at a distance of 24 F from each other[16] and the third point charge is midway between the two fragments. In the case of binary fission the α particle is bound to fragment 2. Hence the (external) electrostatic energy available in binary fission has the form

$$E_B = E_{12} + E_{13}.$$

In the case of LRA fission, the third sphere is not bound to either of the fragments, and hence the external energy is

$$E_{\mathrm{LRA}} = E_{12} + E_{13} + E_{23}.$$

Assuming the α particle to be at a distance of 12 F from either fragment, E_{23} is of the order of 12 MeV. To this we must add the binding energy of the α particle to fragment 2, which is approximately 8.5 MeV for a $Z=48$, $A=124$ nucleus.[31] Assuming the initial energy of the α particle to be 2.5 MeV,[16] we obtain a total of 23.0 MeV for the energy which is required to emit an α particle in the scission process. The total excitation energy which is converted to neutron evaporation in binary fission is 25.4 MeV,[32] and approximately 9 MeV is converted into gamma emission.[33] Hence the average excitation energy available in binary fission of Cf^{252} is 34.4 MeV, and exceeds by 11.4 MeV the average energy necessary for α emission. While in general this excitation energy is distributed among many degrees of freedom, it seems possible that once in 300 fission events an appreciable part of this energy is concentrated in those degrees of freedom which lead to the emission of the α particle. However, it would follow that there is essentially no neutron evaporation associated with LRA fission, whereas Apalin *et al.*[34] measured neutron emission in LRA fission produced by thermal neutrons on U^{235} and found $\bar{\nu}=1.77\pm0.09$ for LRA fission, as compared with $\bar{\nu}=2.45$ for binary fission. Assuming the ratio $\bar{\nu}(\mathrm{LRA})/\bar{\nu}(\mathrm{binary})$ in Cf^{252} to be the same as for $U^{235}+n$, and the gamma energy to be reduced by the same factor, we find that the total excitation energy for LRA fission of Cf^{252} is 24.9 MeV. Thus we have for the difference in excitation energy between LRA and binary fission:

$$E^*(\mathrm{LRA}) - E^*(\mathrm{binary}) = 23.0 + 24.9 - 34.4 = 13.5 \text{ MeV}.$$

We reach similar conclusions from the comparison of the *kinetic* energy in LRA and binary fission. We have seen that the difference in electrostatic energy is 12 MeV and to that we must add the initial kinetic energy of the α particle (2.5 MeV), and hence for the same scission configuration the total kinetic energy in LRA fission should be larger by 14.5 MeV than that of binary fission. The actual difference is approximately 3.0 MeV.[5] Hence the initial electrostatic energy in LRA fission with the α particle removed is smaller by 11.5 MeV than that in binary fission. This value is fairly independent of our particular choices for the scission configuration. Thus a smaller distance between the fission fragments at scission would increase E_{23}, but would decrease the initial energy of the α particle needed in order to fit the experimental distribution. Comparing this number with our estimate based on $\bar{\nu}(\mathrm{LRA})/\bar{\nu}(\mathrm{binary})$ in $U^{235}+n$, we find that the neutron ratio for Cf^{252} is apparently somewhat smaller than that quoted for U^{235}. The difference in the two estimates may also be the result of an inaccurate estimate of the α-particle binding energy, which we assumed to be 8.5 MeV.

We thus conclude that the average scission configuration for LRA fission corresponds to a binary configuration with an electrostatic energy which is lower by 12 MeV or by 6% than the average electrostatic energy in binary fission. In other words the *average distance between the two fragments at scission for LRA fission is larger by 6% than the average distance in binary fission.*[35]

[31] A. G. W. Cameron, Atomic Energy of Canada, Ltd. Report No. CRP 690, 1957 (unpublished).

[32] H. R. Bowman, S. G. Thompson, J. G. D. Milton, and W. J. Swiatecki, Phys. Rev. **126**, 2120 (1962).

[33] H. R. Bowman and S. G. Thompson, in *Proceedings of the Second United Nations International Conference on the Peaceful Uses of Atomic Energy, Geneva, 1958* (United Nations, Geneva, 1958), Vol. 15, p. 212.

[34] V. F. Apalin, Y. P. Dobrynin, V. P. Zakharova, I. E. Kutikov, and L. A. Mikaelyan, At. Energ. (USSR) **7**, 375 (1959) [English transl.: Soviet J. At. Energy **7**, 853 (1961)].

[35] Halpern (Ref. 6) estimates the difference in the average distance to be 13%. His estimate is based on the assumption that the scission configuration in binary fission may be approximated by two point charges, whereas the scission configuration in LRA fission is approximated by three point charges. We, on the other hand, have assumed that the scission configuration is in both cases to be approximated by three point charges, with the difference that in binary fission the α particle is bound to fragment No. 2 and hence the external electrostatic energy E_{23} is zero. It may be argued that immediately after scission occurs the neck is rapidly pulled into the fragments, and hence a two-point charge picture is a better approximation of the scission configuration in binary fission. This view is based on the assumption that the motion of the neck immediately after scission is much faster than the motion of the centers of the fission fragments. However, it seems that at the moment of scission the fragment centers are already moving with approximately one-half of their final velocity, whereas presumably the center of the neck near the point of rupture is almost stationary at the moment of scission. The assumption that the "pulling in" motion of the neck is slow compared to the fragment motion is thus believed to be a better approximation.

The difference of 12 MeV in the electrostatic energy between the two scission configurations is equal to the standard deviation of the kinetic-energy distribution in binary fission.[8] Therefore, the difference in the distance between the two fragments at scission for LRA and binary fission is equal to the standard deviation of the scission distance distribution. In other words, in 15% of the binary fission events, the distance is larger than the average distance in LRA fission. These considerations thus further support our earlier conclusions about the great similarity of the two fission processes.

The results presented in this paper indicate that LRA fission may provide a more direct as well as a more sensitive tool for the study of the nuclear configuration at scission than the study of neutron emission from the fragments. However, the interpretation of the LRA-fission data is more difficult and must be aided by detailed trajectory calculations.

ACKNOWLEDGMENTS

The experiment was carried out while the author was a guest of the Lawrence Radiation Laboratory, Berkeley. He wishes to thank Professor I. Perlman and Dr. S. G. Thompson for their hospitality. The author also wishes to thank Dr. S. G. Thompson, H. R. Bowman, and M. Nakamura for the invaluable help they have extended to him during all phases of the experiment. Finally, he wishes to acknowledge many valuable discussions with E. Nardi, Dr. W. J. Swiatecki, Professor I. Halpern, Professor I. Dostrovsky, and Dr. J. R. Nix.

APPENDIX I: CALIBRATIONS AND CORRECTION PROCEDURES

We describe here briefly the calibration and correction procedures used in obtaining the various angular and energy distributions.

A. Fission-Fragment Energy Calibration

During each experimental run a number of calibration runs were made, normally once a day. In a calibration run, binary coincidences were recorded under conditions identical with those of the triple-coincidence arrangement. The number of counts in each calibration run varied between 5×10^3 to 5×10^4 counts. The single-fission-fragment spectra were later fitted with two-Gaussian distributions with the aid of a modified version of the Los Alamos general least-squares fitting program.[21] The two peak positions determined the gain of the system (in MeV/channel) and the exact zero position. The zero position was affected by a number of factors, namely, the electronic pedestal of the experimental system, the energy loss in the source foils, and, most important, the well-known energy defect of the solid-state detectors. Both the energy loss in the source foils and the energy defect of the detectors were assumed to be independent of the fragment energy. This approximation is certainly justified for the energy loss in the source foils, but it is less justified for the detector energy defect,[36,37] and it was used because of the lack of knowledge of the energy dependence of this defect at the time.

The accuracy of the energy calibration of the two detectors was checked by comparing the number of counts such that $E_1/E_2>1$ with the number of counts such that $E_1/E_2<1$. Theoretically the two numbers should be equal, and in practice they were always equal within the statistical accuracy, the error always being less than one percent. [It should be pointed out that this test is not very sensitive to small errors of the gain or zero position in the detector calibration because of the small number of events near $E_1/E_2=1$. Hence small variations of the gain (or zero position) shift only a small number of events from one "half" to the other.]

B. α-Particle Energy Calibration

The energy calibration of the α-particle counter was made with the aid of an $Es^{253}+Am^{241}$ source which was brought in front of the α-particle detectors instead of the gold absorption foil. An α-particle detector calibration was performed after each fission-fragment-detector calibration. A higher gain position of the amplifier (which increased the gain by approximately a factor of 3) was used for the calibration so as to check the linearity of the multidimensional analyzer in the energy region of greatest interest. With the aid of the two calibration points, the energy loss due to the window of Li-drifted solid-state detectors was determined to be 0.23 MeV.

The thickness of the absorber foils was obtained by weighing them and measuring the area. The energy loss in the foils as a function of α-particle energy was taken from the compilation of Atkinson and Willis.[38] In order to recreate the original smooth energy distribution which had been quantized by the analog-to-digital converter (ADC) of the analyzer, a random number between 0 and 1 was added to the pulse height of the three dimensions of each event as it was read from the magnetic tape into the computer memory. The energy loss corresponding to the noninteger pulse height was then added. However, even the "randomized" α-particle energy distribution obtained in this fashion is not smooth but has a staircase shape. This resulted in some scatter in the points of the resultant distributions when corrected for the energy loss in the Au foil, particularly at the low-energy end where the energy loss corrections are a very steep function of the initial energy. This explains the certain amount of scatter at the low-energy end of the α-particle energy distribution shown in Fig. 3.

[36] H. G. Britt and H. E. Wegner, Rev. Sci. Instr. **34**, 274 (1963).
[37] H. W. Schmitt, W. E. Kiker, and C. W. Williams, Phys. Rev. **137**, B837 (1965).
[38] J. H. Atkinson, Jr., and B. H. Willis, University of California Radiation Laboratory Report No. 2426 (rev.), 1951, Vol. II (unpublished).

Additional reasons for the scatter are inaccuracies in the energy-loss corrections and statistical scatter. There was no evidence for any structure in the uncorrected α-particle energy distribution.

C. Correction for Finite Size of Counters and Source

The counter and source geometry in this experiment was a rather complicated one. Each counter consisted of two circular detectors, one on top of the other, at a slight angle to each other (each detector plane was perpendicular to the line from its center to the center of the source). The source was a circular disk at 30° to the plane of the fission fragment detectors and at any of various angles with respect to the α-particle detector. In the literature, several counter-source geometries have been worked out. Rose[39] discussed in detail the geometry of the two circular counters at angle θ with respect to each other facing a point source. Feingold and Frankel[40] discussed the more general situation and worked out in detail the corrections for circular and rectangular detectors facing a line source. These corrections are already fairly complicated and always involve "mixing corrections" (i.e., the correction terms for the various terms in the polynomial expansion are dependent on the magnitude of the other terms).

Unlike the situation in gamma-gamma correlation experiments, the determination of the exact shape of the angular distribution was not considered to be of primary importance. (This situation may change once detailed calculations are performed for the LRA-fission process.) Of the geometries discussed above, the closest one to our experimental arrangement consists of rectangular counters with a line source. However, even this geometry does not represent the experimental situation very well. It was therefore decided to use only the zero-order terms of this correction (i.e., only terms with $m=0$). Our procedure is therefore equivalent to first substituting for the actual geometry an equivalent rectangular counter-line source geometry, and then substituting for this geometry an equivalent circular counter-point source geometry. The middle step served only for obtaining a better estimate of the diameter of the circular detectors. The equivalent diameters obtained by this procedure were approximately 15 mm for the α-particle counter and 12 mm for the fission-fragment counter. (The fission-fragment detector correction was applied only once, since theoretically the second fission fragment does not add to the experimental width.)

The angular distributions were thus obtained in the following way: The "uncorrected" angular distributions as a function of other parameters of interest (e.g., R, E_F, E_α) were corrected for variations in the singles rate as a function of angle. (These variations differed slightly for each run because of slightly different sizes of detectors, etc.) The curves obtained for all the experimental runs were then added to give better statistics. One such "uncorrected" curve is shown in Fig. 2. Next the uncorrected angular distribution was fitted to a Legendre polynomial expansion

$$N_u(\theta,X_1,X_2)=\sum_{l=0}^{n}\alpha_l P_l(\cos\theta),$$

by a least-squares fit. Next the corrections were applied to the coefficients

$$\beta_l=\alpha_l C_F{}^l C_l{}^l,$$

$C_F{}^l$ being the correction for the fission-fragment counter and $C_\alpha{}^l$ the correction for the α-particle counter. Finally the corrected angular distribution was obtained:

$$N_c(\theta,X_1,X_2)=\sum_{l=0}^{n}\beta_l P_l(\cos\theta).$$

The program calculated N_c for all values of n up to $n=10$, but for the distributions shown $n=5$ was used. Larger n had little effect on the main peaks of each distributions, whereas the outer wings did not seem to converge to an asymptotic value even at large n. Whenever the value of a distribution started to show large variations with increasing n, no values are given for the distribution at these angles in the figures. This is the reason that there are a number of graphs which were not continued to angles θ_L above 105° or 110°. This terminating procedure is of course highly arbitrary and therefore even points shown on the outer edge of the distribution cannot be considered well established. Yet, while the above corrections are at best a first approximation to the true corrections, the errors in the positions of the *peaks* in the distribution due to our procedure are almost certainly within the experimental error of ±1°, and we estimate the possible error in the widths of the peaks to be less than 10%.

In order to check the uniquencess of our angular correction procedure we calculated the distribution $N(\theta_L,E_F)$ (Fig. 13) by summing $N(\theta_L,E_F,E_\alpha)$ (Fig. 14) over all values of E_α and also by summing $N(\theta_L,E_F,R)$ (Fig. 12) over all values of R. The two distributions agreed with each other within the statistical uncertainty.

APPENDIX II: THE EFFECT OF THE α-PARTICLE RECOIL ON THE FISSION-FRAGMENT ENERGY RATIO

The relation between the fission-fragment energy ratio and the mass in LRA fission (neglecting the effect of neutron emission) is obtained from the condition that the total momentum in the direction of the light fragment be zero:

$$(m_L E_L)^{1/2}=(m_H E_H)^{1/2}\cos\theta_R-(m_\alpha E_\alpha)^{1/2}\cos\theta_L. \quad \text{(A1)}$$

[39] M. E. Rose, Phys. Rev. **91**, 610 (1953).
[40] A. M. Feinfold and S. Frankel, Phys. Rev. **97**, 1025 (1955).

Here m_L, m_H, and m_α are the masses of the light and heavy fragment and the α particle, respectively, and E_L, E_H, and E_α are their final energies

θ_R is the recoil angle of the fission fragments

$$\theta_R=\theta_F-\pi, \quad \text{(A2)}$$

where θ_F is the angle between the final directions of the light and heavy fragments.

The recoil angle θ_R may be obtained from the condition that the total momentum perpendicular to the direction of the light fragment be zero:

$$(m_H E_H)^{1/2}\sin\theta_R=(m_\alpha E_\alpha)^{1/2}\sin\theta_L,$$

yielding

$$\sin\theta_R=\left(\frac{m_\alpha E_\alpha}{m_H E_H}\right)^{1/2}\sin\theta_L. \quad \text{(A3)}$$

The relation between the fission-fragment energy ratio and the mass ratio is obtained from Eq. (A1):

$$\frac{E_L}{E_H}=\frac{m_H}{m_L}\left[\cos\theta_R-\left(\frac{m_\alpha E_\alpha}{m_H E_H}\right)^{1/2}\cos\theta_L\right]^2=a\frac{m_H}{m_L}. \quad \text{(A4)}$$

For mean values of E_α and E_F ($E_\alpha=16$ MeV, $E_F=168$ MeV), the maximum value of the recoil angle θ_R is $\theta_{R\,\max}\simeq 4.5°$. [This maximum angle is obtained for $\theta_L=92.25°$, i.e., for $2\theta_L-\pi=\theta_R$. The correction factor $(a-1)$ is exactly zero at this angle.]

We find that the mass-ratio correction factor $(a-1)$ is always negligible for $\theta_L=90°$ [$a(90°)\simeq 0.997$]. For the range of angles θ_L of interest in the current investigation, we find that the correction factor changes (approximately linearily with the angle θ_L) from $(a-1)\simeq -7.5\%$ for $\theta_L=60°$ to $(a-1)\simeq +7.5\%$ for $\theta_L=120°$. In other words, at $\theta_L=60°$ the α-particle recoil causes the energy ratio to be smaller by approximately 7.5% than the mass ratio, whereas at $\theta_L=120°$ the energy ratio is larger than the mass ratio by approximately the same amount.

The present experiment measured the kinetic energies of the two fragments and hence the energy ratio $R_E=E_L/E_H$. In order to obtain the various distributions as a function of the mass ratio $R=m_H/m_L$ (again neglecting the effect of neutron emission), the energy ratio obtained for each event is multiplied by the factor a^{-1} of the given event. For this purpose a may be approximated by

$$a\simeq\left\{1-\left[\frac{m_\alpha}{m_H+m_L}\frac{E_\alpha(E_1+E_2)}{E_1E_2}\right]^{1/2}\cos\theta_L\right\}^2. \quad \text{(A5)}$$

Equation (A5) involves only known or measured quantities. The above procedure assumes the angle θ_L to be accurately known. However, in the present experiment the angular resolution was rather poor. This fact is of no importance for other aspects of the analysis, since it can be corrected for in the usual manner (see Appendix I). However, it complicates the transformation from energy ratio to mass ratio, since the angular distribution is peaked at $\theta_L\simeq 82°$ and falls off rapidly for smaller and larger angles, whereas the correction factor $(a-1)$ is zero at $\sim 92°$ and its absolute value increases for smaller and larger angles. If the nominal angle θ_L of the detector is used for this transformation, it will cause on the average an overestimate of the mass ratio for angles $\theta_L<90°$ and an underestimate for the mass ratio for $\theta_L>90°$, i.e., the α-particle recoil effect is overcompensated for. Since $N(R_E)$ (Fig. 5) decreases sharply with R_E for $R_E>1.4$, this overcompensation therefore results in an overestimate of the number of events with $R>1.4$ at small θ_L. The number of events with $R<1.2$ is overestimated for similar reasons at large θ_L. This is probably the reason for the "flattening off" of curve A, Fig. 10 at high θ_L, and of curve C, Fig. 11(d) at low θ_L. Similarly, the value of curve D, Fig. 10 at $\theta_L=60°$ is probably too large.

APPENDIX III: BACKGROUND DUE TO REACTIONS OTHER THAN LRA FISSION

Among the graphs which were shown in this paper there are several curves which show a very wide angular distribution on which a peak is superimposed. These curves are associated with high fission-fragment energies, mostly in the region $E_F>190$ MeV [e.g., curves E of Figs. 13, 14(b), and 14(c)]. Our data show that only 5% of all LRA-fission events have a fragment energy above $E_F=190$ MeV, whereas 26% of all binary-fission events of Cf^{252} have a fragment energy above this limit. These numbers indicate that the wide angular distributions in these curves may be due to random-coincidence events and other background associated with binary-fission events. Thus, for example, the total measured coincidence rate between binary-fission events and α particles from LRA fission was 4% of the true fission rate at an angle of $\theta_L=90°$. The random-coincidence rate for $E_F>190$ MeV was therefore $(0.26/0.05)\times 0.04=0.21$ of the true rate at $\theta_L=90°$. It seems, however, that for some curves the isotropic background is higher than this figure, and therefore random coincidences alone probably cannot explain the wide experimental distributions. It is thus of interest to look for other possible causes of this effect.

In searching for other possible causes for the wide angular distributions above $E_F=190$ MeV, we must take into account the fact that the α-particle energy distribution for this region does not greatly differ from the total α-particle energy distribution, except for a shift of approximately 1 MeV towards lower energies. Also, the depletion layer of the α-particle detectors had a depth of approximately 0.5 mm, and protons with energy above 10 MeV were not stopped in the depletion layer. Triple-fission events in which particles heavier than α particles are emitted are probably associated with lower values of E_F than in LRA fission. Moreover,

there seems to be no reason to expect a much wider angular distribution for these particles.

(n,α) reactions produced by fission neutrons in the Au absorber, in the chamber walls, and in the α-particle detectors produce α particles below our lower limit of $E_\alpha = 10$ MeV. Nuclear reactions of fission fragments in the source backing or in the fission-fragment detectors cannot account quantitatively for the observed background.

Let us finally examine the possibility that the almost isotropic distributions are due to α particles evaporated from excited fission fragments. Such α particles would have a kinetic energy above $E_\alpha = 10$ MeV and an angular distribution which is almost isotropic (it is somewhat peaked in the direction of the fission fragments). In order to account for the "background" the α-particle evaporation probability in binary fission with $E_F > 190$ MeV must be approximately 10^{-3}. In order to check this possibility, an evaporation calculation was performed for several representative fission fragment nuclei. The evaporation program of Dostrovsky *et al.*[41] was used with the level-density parameter $a = A/20$. The mass ratio for which α-particle emission was found to be most likely lies near the high-mass peak ($A \simeq 145$). Below this region the α-particle binding energy is too large, whereas for heavier nuclei the Coulomb barrier prevents α-particle emission. (On the basis of similar argument, Feather[42] concludes that all α particles in LRA fission are emitted from the heavy fragment.) The probability of α-particle emission from a $Z = 56$, $A = 144$ nucleus with an excitation energy of $E^* = 20$ MeV was calculated to be less than 10^{-4}. The probability increases to. $(1.7 \pm 0.4) \times 10^{-3}$ for an excitation energy of $E^* = 40$ MeV. The average excitation energy in the form of prompt neutrons is $E^* \simeq 10$ MeV for an $A = 145$ fragment.[26] We may therefore conclude that normal α-particle evaporation from the fission fragments cannot explain the wide distributions. However, the fission fragments are very highly deformed when scission occurs, and α-particle emission may be enhanced in the time interval preceding the establishment of the statistical equilibrium which is assumed in the evaporation calculations.

It should again be emphasized that these considerations refer only to a very small fraction of the LRA-fission events. As already mentioned, our data show that almost all α particles are emitted within 10^{-21} sec of the moment of scission.

[41] I. Dostrovsky, Z. Fraenkel, and G. Friedlander, Phys. Rev. **116**, 683 (1959).

[42] N. Feather, Proc. Roy. Soc. (Edinburgh) **66A**, 192 (1964).